A MODEL OF BACTERIAL SUPERINFECTION IN AN INFLUENZA-INFECTED HOST

by

Sherry B. Linn

B.S. in Mathematics, Millersville University, 2008

Submitted to the Graduate Faculty of

the Arts and Sciences in partial fulfillment

of the requirements for the degree of

Master of Science

University of Pittsburgh

2011

UNIVERSITY OF PITTSBURGH

ARTS & SCIENCES

This thesis was presented

by

Sherry B. Linn

It was defended on

March 18, 2011

and approved by

Prof. David Swigon, Department of Mathematics

Prof. Gilles Clermont, Department of Critical Care Medicine

Prof G. Bard Ermentrout, Department of Mathematics

Prof. Jonathan Rubin, Department of Mathematics

Thesis Advisor: Prof. David Swigon, Department of Mathematics

A MODEL OF BACTERIAL SUPERINFECTION IN AN INFLUENZA-INFECTED HOST

Sherry B. Linn, M.S.

University of Pittsburgh, 2011

Bacterial pneumonia is a common complication of influenza A infection. We create an ODE model of bacterial infection with state variables representing the respective levels of bacteria, impaired and active neutrophils, and the anti-inflammatory molecule interleukin 10 (IL-10). After fitting the parameters, we obtain a model that demonstrates bistability between states of health and chronic bacterial infection. The fitted model also closely reproduces IL-10 data obtained from a model of mice inoculated with a strain of influenza A virus. Additionally, we develop a different model similar to the first but with stochastic intake of bacteria to represent the inhalation of small amounts of bacteria into the lungs many times daily. We find a set of parameters for which the second model produces a fit to the IAV IL-10 data.

TABLE OF CONTENTS

LIST OF TABLES

LIST OF FIGURES

1.0 INTRODUCTION

The term superinfection refers to the situation in which a pathogen infects a host while the host is already battling an infection. A well-known example is the occurrence of bacterial pneumonia shortly after influenza infection. This is the main cause of death from seasonal influenza, which claims 35,000 lives annually in the United States of America. There are many possible causes of superinfections. One theory is that the primary infection elicits an immune response, creating a window of time during which the immune system is not at the resting equilibrium state of health and is susceptible to infection by another pathogen. This window occurs due to neutrophil paralysis, the prevention of neutrophil migration to the site of bacterial infection by a canonical anti-inflammatory molecule, IL-10.

It is well documented that the seasonal flu has a higher mortality rate among the elderly population (aged 65 year or older) than it does among younger individuals. In a study by Toapanta et al. that sought to better understand this phenomenon, aged and adult mice were infected with a strain of IAV (A/Puerto Rico/8/34) and then monitored for differences in immune dynamics [11]. In both aged and adult mice; weight loss, mortality, and virus titer were monitored. In addition, cells of the innate and adaptive immune response, cytokines and chemokines produced by immune cells were all analyzed and counted.

Although unmentioned in their manuscript, Toapanta et al. measured levels of IL-10 (pg/mL) for the experiment discussed in [11]. Figure 1 shows levels of IL-10 taken for a sublethal case in IAV-infected adult mice up to 19 days post-infection. The figure also shows virus titer data from the mice during the same span of days. The first and larger hump in the IL-10 data is due to the host immune response to the IAV infection. As described in Section 2.2.3, the host immune response to pathogenic invasion is a pro-inflammatory wave shortly followed by an anti-inflammatory wave, which we observe in the first peak in the

IL-10 data. Note the increase in IL-10 on Day 11 despite the absence of virus after Day 9. We hypothesize that this unexpected hump in IL-10 levels is due to an unintended secondary bacterial infection facilitated by the inoculation of the mice with IAV.

Specifically, we believe that the facilitation of the bacterial infection can be explained as a result of the immune response to the IAV infection. The first peak in IL-10 data marks the anti-inflammatory wave initiated by the IAV infection, during which neutrophil paralysis is known to occur. We posit that the temporary paralysis of neutrophils allows the bacteria to reproduce and spread; the neutrophils are not at the site of infection to attack the bacteria and to signal other pro-inflammatory effectors to the infection site.

Section 2 provides an introduction to the topics of influenza infection, pneumonia, superinfection, and immune response. It also gives a brief review of literature on research related to viral-bacterial superinfections and IAV-bacterial pneumonia superinfections.

In Section 3, we analyze the dynamics of a two-equation ordinary differential equation (ODE) model of interactions between bacteria and activated neutrophils. We then develop a four-equation model based on the two-equation model, this time also including interactions involving IL-10 and paralyzed neutrophils. We take the IL-10 output from the IAV infection to be the difference between the linear interpolation of the first seven data points and the IL-10 steady state level. The IL-10 output from the bacterial infection is determined by the model dynamics. We then find a set of parameters for which the total IL-10 matches the linear interpolation of all given IL-10 data points.

In Section 4, we develop a model similar to that in the previous section, using stochastic inhalation of bacteria many times per day, instead of using a constant rate of bacteria inhalation, into the lower respiratory tract. Because the IL-10 data comes from several mice, we find the average total IL-10 produced by the system, and compare it to the given IL-10 mouse data. We find a set of parameter values for which the system's average total IL-10 is a close match to the linear interpolation of the ten given IL-10 data points.

In Section 5, we conclude by discussing possible extensions of research involving the model with stochastic bacteria inhalation.

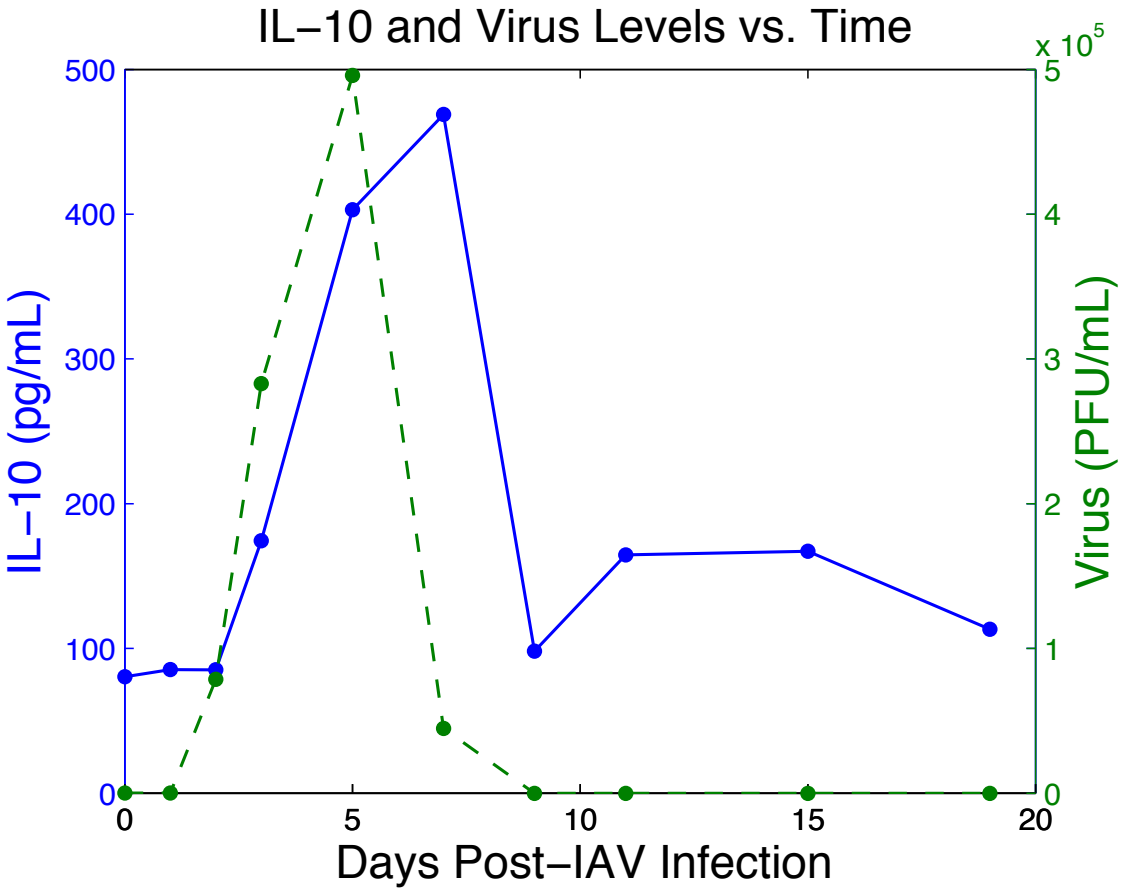

Figure 1: The 10 data points of IL-10 levels (blue) and viral titer levels (green) in IAV-infected mice collected by Toapanta et al. over the course of 19 days post infection. The lines between data points indicate piecewise linear interpolation based on the given data.

2.0 BACKGROUND AND MOTIVATION

2.1 IAV AND BACTERIAL PNEUMONIA

The influenza virus is known globally as a public health concern and a hindrance to society, responsible for high levels of work absenteeism, productivity losses, and the overwhelming of medical facilities caused during peak influenza illness periods. The symptoms of influenza infection include fever, chills, headache, muscle pain, fatigue, and nasal congestion. Influenza can be fatal when it leads to lethal complications. Annually, seasonal influenza epidemics result in 250,000-500,000 deaths and 3-5 million cases of severe illness worldwide [14]. These figures do not include pandemics; the 1918, 1957, and 1968 influenza pandemics had estimated death tolls of 40-50 million, 2 million, and 1 million people, respectively [15]. There are three types of influenza virus: influenza A, B, and C. Of these three types, influenza A virus (IAV) is the most virulent. To this point, the 1918, 1957, 1968, and 2009 pandemic strains of influenza were of type A, making IAV a topic of research across many disciplines, including immunology, microbiology, and mathematical biology.

Pneumonia is a respiratory condition often characterized by the filling of alveoli with inflammatory fluid interfering with gas exchange. This fluid accumulation is the direct effect of vasoactive agents produced by inflammatory cells, such as neutrophils, in their efforts to contain and eradicate invading bacteria. In severe cases of pneumonia, gas exchange is so impaired that animals die and humans require mechanical ventilatory support in intensive care units and incur substantial mortality, as well. Pulmonary inflammation associated with pneumonia can also lead to pleural effusion, empyema (infected effusion), lung abscesses, and acute lung injury (ALI). ALI is a condition in which pulmonary inflammation persists irrespective of the presence of bacteria. Pneumonia is a major cause of death in the elderly,

infants and young children, and individuals with chronic illness. *Streptococcus pneumoniae* is the bacteria most commonly associated with bacterial pneumonia infections [2], [5], [8]. *Staphylococcus aureus* and *Haemophilus influenzae* are other bacteria known to cause pneumonia.

There is much evidence of IAV-bacterial pneumonia superinfections. A recent study by Morens et al. of autopsy data and tissue samples from 58 victims of the 1918 IAV pandemic found common respiratory-tract bacteria and other histological indicators of acute bacterial pneumonia infection in most of the samples. This discovery led the authors to conclude that the majority of 1918 IAV pandemic deaths were directly caused by secondary bacterial pneumonia as opposed to being caused by the IAV infection itself [8]. The same study concluded similar results with respect to the 1957 and 1968 IAV pandemics.

There is also evidence that correlates bacterial pneumonia with severe illness in patients infected with 2009 pandemic H1N1 (H1N1 pdm). The Center for Disease Control (CDC) received lung tissue samples from 77 American victims of H1N1 pdm, collected from May 1, 2009 to August 20, 2009 [13]. Analysis of these samples exhibited evidence of concurrent bacterial infection in 22 of the victims. *S. pneumoniae* was the most prevalent bacteria in this study, found in 10 of the 22 victims showing concurrent bacterial infection. Palacios, et al. conducted a similar study of Argentineans infected with H1N1 pdm [9]. They studied 199 cases of patients diagnosed with H1N1 pdm infection; 160 cases were diagnosed as mild and 39 as severe. *S. pneumoniae* was found in the patient's respiratory tract in 62 of the H1N1 pdm cases, 22 of these cases involving severe IAV infection and the remaining 40 being mild. From this data, the study concluded that the presence of *S. pneumoniae* in H1N1-pdm infected patients is a significant indicator of severe illness.

The given examples suggest a correlation in severity of illness in IAV-infected patients and secondary bacterial infection, i.e. that the lethality of IAV is increased in cases in which bacterial pneumonia is contracted. Experiments by McCullers et al. further support the existence of such a relationship between IAV and bacterial pneumonia [7]. To test the efficacy of antiviral treatments in cases of bacterial pneumonia following IAV infection, McCullers et al. inoculated four groups of six mice with *S. pneumoniae*. Three of these groups were also inoculated with the same strain of IAV seven days prior to inoculation with *S. pneumoniae*.

These three groups were each given one of three antiviral treatments: oseltamivir, rimantidine, or a placebo. Oseltamivir inhibits neuraminidase (NA), while rimantidine inhibits the M2 proton channel protein (M2). If the mice exhibited signs of pneumonia, they were treated with the antibiotic ampicillin. All mice that were inoculated with only *S. pneumoniae* survived and five of the six mice in the oseltamivir group survived, while none of the mice in the rimantidine group survived and none of the mice in the placebo group survived. There is much evidence that influenza increases adherence of bacteria to epithelial cells. The authors found that inhibition of NA reduces the adherence of *S. pneumoniae* to alveolar basal epithelial cells, whereas inhibition of M2 does not. This agrees with the results that mice coinfected with IAV and *S. pneumoniae* that were treated with oseltamivir and ampicillin had a greater survival rate compared to those treated with rimantidine and ampicillin. The results of this experiment suggest that *S. pneumoniae* is not fatal by itself, but that infection with IAV followed by infection with *S. pneumoniae* can be fatal, supporting that influenza affects the pathogenesis of bacterial pneumonia in such a way that *S. pneumoniae* is able to overwhelm the host before specific immune responses can develop.

In another experiment by McCullers et al., 30 mice were infected intranasally with IAV and then inoculated with *S. pneumoniae* seven days later [7]. 22 of the mice were treated with oseltamivir and ampicillin. All mice given both the anti-viral and antibiotic treatments survived. Seven of these 22 mice developed pneumonia and had visually cleared the pneumonia by the eighth day post *S. pneumoniae* infection. The other eight of the 30 mice were treated with ampicillin alone. All eight of these mice developed pneumonia and died, even though six of these eight mice had visibly cleared the pneumonia before death. On the basis of this experiment, the authors hypothesized that treatment with oseltamivir delays the onset and slows the progression of bacterial pneumonia by lessening the severity and duration of IAV. This in turn could alter the pathogenesis of bacterial pneumonia so that the clearance of *S. pneumoniae* is enough to bring the mice back to health.

The findings of these experiments by McCullers et al. show that bacterial pneumonia is more likely to develop in an *S. pneumoniae*-infected host recovering from an IAV infection than it is to develop in a host battling a *S. pneumoniae* without a proceeding IAV infection. This, in addition to the correlation between severity in H1N1 pdm-infected patients and

secondary *S. pneumoniae* infection found in the study by Palacios et al., demonstrates that IAV and *S. pneumoniae* have a synergistic relationship that leads to an outcome worse than the outcome of the host had it been infected with only IAV or only *S. pneumoniae*.

According to Bakaletz, the presence of IAV is often necessary for bacterial infection to establish itself in the lower respiratory tract [2]. The well-documented prevalence of bacterial pneumonia following IAV infection and the increased mortality that secondary bacterial pneumonia can lead to in IAV-infected patients has led to research as to the possible causes of this phenomenon.

2.2 VIRAL POTENTIATION OF BACTERIAL INFECTION

2.2.1 Examples

It is important to note that the permissive relationship between IAV and bacterial pneumonia is not the only documented example of viral infections amplifying the potency of bacterial infections when the two infections occur within close chronological proximity to one another. Bakaletz points out that sinusitis is often observed after rhinovirus, influenza, adenovirus, or parainfluenza virus infections [2]. Also, in an experiment by Giebink in which chinchillas were either infected with IAV alone, *S. pneumoniae* alone, or both IAV and *S. pneumoniae*, IAV was found to potentiate otitis media infection [2]. Suzuki and Bakaletz observed through experiment with a similar model that adenovirus potentiates *Haemophilus influenzae*; whether the subjects were inoculated with adenovirus before or after infection with *H. influenzae*, both the severity and incidence of otitis media increased [2]. In the 1940s, many studies were conducted on animal models in which infection with influenza virus followed by infections with any of several pneumopathic bacteria resulted in a higher occurrence of disease, shortened time to death, or higher death rate [8].

2.2.2 Causes

Much research has been conducted in order to unearth the causes of and mechanisms responsible for viral potentiation of bacterial infection. Goldstein et al. looked to formulate a correlation between bacterial infections and viral infections that precede them through an experiment in which some mice were immunized against Mengo-37A, a weak strain of encephalomyocarditis (ECM) virus, while the remaining mice in the experiment were not [4]. All mice were then either inoculated with Columbia-SK, which is a virulent strain of ECM virus, Mengo-37A, or a placebo. Finally, all mice were inoculated with *Staphylococcus aureus*. The immunized mice that were infected with either strain of the ECM virus experienced respiration and pulmonary bactericidal activity similar to that of the control mice. Non-immunized mice that were infected with Columbia-SK were observed to have bactericidal dysfunction worse than that observed in non-immunized mice infected with Mengo-37A. This experiment connects virulence of the preceding virus with an inability to clear a secondary bacterial infection. It also provides an example of how the physiological effects of a viral infection can yield changes that potentiate a bacterial infection.

There are other possible reasons as to why viral-bacterial superinfections tend to be more pathogenic than the bacterial infection would be without the preceding viral infection. For example, IAV and other viral infections in the respiratory tract result in damage to respiratory epithelia, which exposes the basement membrane as well as surfaces of regenerating cells. These exposed surfaces are possible binding sites for bacteria, allowing the bacteria to populate in the respiratory tract where they would normally not be able to do so. Viral infection of epithelial cells that have not already been destroyed can also lead to the creation of potential bacterial binding sites, in this case on the infected host cell [2]. For example, the influenza virus has been found to increase the adherence of bacteria to epithelium in vitro, in animal models, and in humans [7]. Destruction of respiratory epithelium also negatively impacts the ability of cilia to move particles, bacteria, and fluid out of the lower respiratory tract [2]. The lower respiratory tract is thought to be sterile of bacteria [2]. The mucociliary escalator is the primary defense against bacteria that contaminate the upper respiratory tract and is what keeps the lower respiratory tract virtually free of bacteria; however, damage to

the cilia allows bacteria the opportunity to populate the lower respiratory tract.

McAuley et al. focused on PB1-F2, a proapoptotic IAV protein found in the pandemic 1918 strain, as a possible factor in the lethality of the 1918 flu pandemic via secondary bacterial pneumonia [6]. They conducted an experiment involving a wild-type strain (WT) and an isogenic strain (mut) of the mouse-adapted influenza A/Puerto Rico/8/34 (PR8) strain. The mut PR8 was engineered so as to significantly reduce the expression of PB1-F2. Two groups of six mice were infected with either the WT or mut viruses and then inoculated with *S. pneumoniae* seven days later. The group of mice infected with the WT virus experienced greater weight loss, incidence of bacterial pneumonia, and mortality than the group of mice infected with the mut virus. The control mice, which were not inoculated with *S. pneumonia*, survived regardless of whether they were infected with the WT virus or the mut virus. The authors concluded that PB1-F2 is pro-inflammatory to the host, can enhance the virulence of the strain of IAV that contains it, and facilitates secondary bacterial pneumonia. They suggested that the apoptosis of host cells caused by PB1-F2 sets off a positive feedback loop of inflammatory cytokines, which is amplified by the presence of bacterial pneumonia. This, in turn, enhances the inflammatory response to the IAV in the lungs.

From the account of immunopathological death described by McAuley et al., it is clear that the immune response induced by viral infection is important to consider when investigating possible reasons for the synergistic relationship of viral-bacterial superinfections. In the second experiment by McCullers et al. described above, six out of the eight mice treated with only antibiotic were able to visibly clear the *S. pneumoniae* from their lungs but nonetheless did not survive the IAV-*S. pneumoniae* coinfection. This also suggests an immunopathological death – an inability for the host to return to health despite the absence of the bacteria that initially caused the pneumonia.

2.2.3 The Immune Response to Infection and Neutrophil Paralysis

The host immune response to acute stress, such as IAV infection, begins with a wave of pro-inflammatory cytokines including interleukin-1 (IL-1), interleukin-8 (IL-8), interferon gamma

(INF-γ), and interferon alpha (INF-α). These cytokines mobilize neutrophils and other immune effectors so as to contain and clear the pathogen. Almost immediately following is a wave of anti-inflammatory cytokines, which inhibit pro-inflammatory cytokines and initiate the healing response. The repression of pro-inflammatory mediators creates a window of opportunity for secondary infections to thrive [1]. The suppression of neutrophil migration to the site of pathogen infection is another possible manner in which viruses can potentiate bacterial infections [2].

Neutrophils are the first line of defense against infection, migrating through blood vessels by chemotaxis in response to the secretion of IL-1, IL-8, INF-α, and INF-γ. The impairment of neutrophil migration to an infection site is known as neutrophil paralysis and is related to the depletion of appropriate cell surface receptors to IL-8 on neutrophils. This phenomenon is a key feature in sepsis, a condition in which a bacterial infection may not be cleared, while the entire system is overwhelmed with inflammation. Interleukin-10 (IL-10) is an anti-inflammatory cytokine that is a major regulator of inflammation and has been found to inhibit cytokine expression, in the lung in particular [10]. In the absence of the secretion of cytokines at the site of infection, neutrophils cannot migrate to the site of infection. IL-10 is also inhibits the ability for neutrophils to phagocytose the bacteria.

The effects of neutrophil impairment and overexpression of IL-10 were studied in an experiment by Sun et al. [10]. Mice were genetically altered with a gene that overexpresses IL-10 in the lungs only when induced with tetracycline. These mice (IL-10 OE) and control mice (WT) were inoculated with *Pseudomonas aeruginosa*. The IL-10 OE mice experienced neutrophil paralysis and increased bacteria counts in comparison to the WT mice. In a different experiment, neutrophil depletion was induced in IL-10 OE mice and in WT mice, resulting in impaired bacterial clearance in both types of mice [10]. The authors concluded that the neutrophil paralysis associated with IL-10 leads to increased bacterial counts, increased inflammation in the lungs, and a higher incidence of mortality.

From the above experiment by Sun et al., it is clear that neutrophil paralysis has detrimental effects in the face of bacterial infection. Neutrophil paralysis has also been observed in patients with leukemia, diabetes, and AIDS, all of which are diseases associated with a high susceptibility to secondary bacterial infection [1].

3.0 MODEL 1: DETERMINISTIC INHALATION OF BACTERIA

In order to test the plausibility of the hypothesis that the second wave of IL-10 observed in the IAV mouse data collected by Toapanta et al. is caused by a secondary bacterial infection, we develop an ODE model containing state variables representative of the quantities of paralyzed neutrophils, N_P, activated neutrophils, N_A, bacteria, B, and IL-10 produced in response to the bacterial infection, I. We will begin by developing a two-equation ODE model representative of the interaction between activated neutrophils and bacteria.

3.1 THE B-N_A SUBSYSTEM

When developing the B-N_A subsystem, we take into account the interactions between bacteria and activated neutrophils shown in Table 1.

In addition to the above reactions, we assume that the presence of bacteria in the respiratory tract recruits activated neutrophils; however, the recruitment rate saturates with

$N_A + B \xrightarrow{\xi} N_A$	B is destroyed at rate ξ when it interacts with N_A.
$N_A \rightarrow$	N_A experiences natural death.
$* \xrightarrow{p} B$	B is inhaled into lower respiratory tract at rate p.

Table 1: A summary of the interactions between B and N_A

the increase of bacteria. For this reason, we represent the recruitment rate of activated neutrophils with a Michaelis-Menten-like term, $\frac{B}{1+sB}$, where $\frac{1}{s}$ is the amount of bacteria for which the recruitment rate reaches its maximum level.

Further, we assume that the bacteria undergo logistic growth, which we represent with the term $k_{pg}B(1-B)$, where k_{pg} is the bacterial growth rate. We represent the removal of bacteria from the respiratory tract via the mucociliary escalator with the term $-\frac{\mu_1 B}{\mu_2+B}$. A saturation term is appropriate since the rate at which this mechanism removes bacteria levels off when the amount of bacteria is above a certain threshold.

These assumptions and the reactions in Table 1 yield the system of equations (3.1) and (3.2).

$$\frac{dB}{dt} = \left(p + k_{pg}B(1-B) - \frac{\mu_1 B}{\mu_2 + B} - \xi B N_A\right)\epsilon_B \tag{3.1}$$

$$\frac{dN_A}{dt} = \left(-N_A + \frac{B}{1+sB}\right)\epsilon_{N_A} \tag{3.2}$$

The variables B and N_A are dimensionless because the correct quantities for the bacteria and neutrophils in the system is unknown. We include the parameters ϵ_B and ϵ_{N_A} for dimensional correctness. For the time being, we will set $\epsilon_B = 1$ and $\epsilon_{N_A} = 1$. We will choose parameters so that all relevant equilibria of System (3.1) - (3.2) are in the first quadrant of the B-N_A plane since negative quantities of bacteria and neutrophils are not possible. In order for the system to be representative of biological phenomena, System (3.1) - (3.2) must exhibit bistability between health and chronic infection for some set of parameters. We define health as the state for which bacteria levels and neutrophil levels are low and at equilibrium. Chronic infection is the state for which bacteria and neutrophil levels are high and at equilibrium. We will first find parameters such that System (3.1) - (3.2) has three equilibria in the first quadrant of the B-N_A plane and then verify that the two outer equilibria are stable, while the middle equilibrium is a saddle point. This will yield the desired bistability.

The equilibria of System (3.1) and (3.2) are located at the intersections of the system's nullclines. We find the nullclines by setting each equation equal to zero and solving for the variable N_A in terms of B. For Equation (3.1), we have

$$\frac{dB}{dt} = 0 \Rightarrow p + k_{pg}B(1-B) - \frac{\mu_1 B}{\mu_2 + B} - \xi B N_A = 0 \tag{3.3}$$

$$\Rightarrow N_A = \frac{-k_{pg}B^3 + k_{pg}(1-\mu_2)B^2 + (p - \mu_1 + k_{pg}\mu_2)B + p\mu_2}{\xi B(B+\mu_2)}. \tag{3.4}$$

Similarly, for Equation (3.2), we obtain

$$\frac{dN_A}{dt} = 0 \Rightarrow -N_A + \frac{B}{1+sB} = 0 \tag{3.5}$$

$$\Rightarrow N_A = \frac{B}{1+sB}. \tag{3.6}$$

Thus the two nullclines of System (3.1) and (3.2) are

$$N_A^1(B) = \frac{-k_{pg}B^3 + k_{pg}(1-\mu_2)B^2 + (p - \mu_1 + k_{pg}\mu_2)B + p\mu_2}{\xi B(B+\mu_2)} \tag{3.7}$$

$$N_A^2(B) = \frac{B}{1+sB} \tag{3.8}$$

To find the equilibria of the System (3.1) and (3.2), we need to identify the points $(B^*,\ N_A^*)$ at which the nullclines (3.7) and (3.8) intersect. The values B^* at which the two nullclines intersect are found by finding the values of B such that

$$\frac{-k_{pg}B^3 + k_{pg}(1-\mu_2)B^2 + (p - \mu_1 + k_{pg}\mu_2)B + p\mu_2}{\xi B(B+\mu_2)} - \frac{B}{1+sB} = 0 \text{ , or}$$

$$f(B) = 0, g(B) \neq 0$$

where

$$f(B) = (-k_{pg}s)B^4 + (k_{pg} - k_{pg}s + k_{pg}s\mu_2 + \xi)B^3 \tag{3.9}$$
$$+ (k_{pg} + ps - s\mu_1 - k_{pg}\mu_2 + k_{pg}s\mu_2 - \mu_2\xi)B^2$$
$$+ (p - \mu_1 + k_{pg}\mu_2 + ps\mu_2)B + p\mu_2, \text{ and}$$

$$g(B) = \xi B(1+sB)(\mu_2 + B) \tag{3.10}$$

$p = 0.0012$	$k_{pg} = 0.05$	$\mu_1 = 0.01$
$\mu_2 = 0.1$	$s = 5$	$\xi = 0.1$

Table 2: For these parameter values, System (3.1) - (3.2) exhibits bistability. Bistability in the model is necessary because the immune system can exhibit both health and chronic inflammation.

We choose $s = 5$ so that the half-maximum value of the saturation term $\frac{B}{1+sB}$ occurs for $B = 0.2$. We select values for the remaining parameters so that bistability is possible. We also want the values of B and N_A at the state of health to be very small and positive, while the state of chronic infection should yield values of B and N_A that are significantly higher than those for the health state. The parameter values in Table 2 satisfy these qualities. The four equilibria of the B-N_A subsystem for the parameter values in Table 2 are displayed in Table 3. (B_3, N_{A3}) has a negative B-coordinate, so we will not consider this equilibrium in our analysis. The nullclines of System (3.1) - (3.2) and the remaining three equilibria can be seen in Figure 2, which was generated with XPPAUT [3]. The code can be found in the Appendix, Section A.1.

$(B_1, N_{A1}) = (0.0580,\ 0.0450)$
$(B_2, N_{A2}) = (0.0902, 0.0621)$
$(B_3, N_{A3}) = (-0.2363, 1.3009)$
$(B_4, N_{A4}) = (0.3881, 0.1320)$

Table 3: The equilibria of System (3.1) - (3.2) for the parameter values in Table 2.

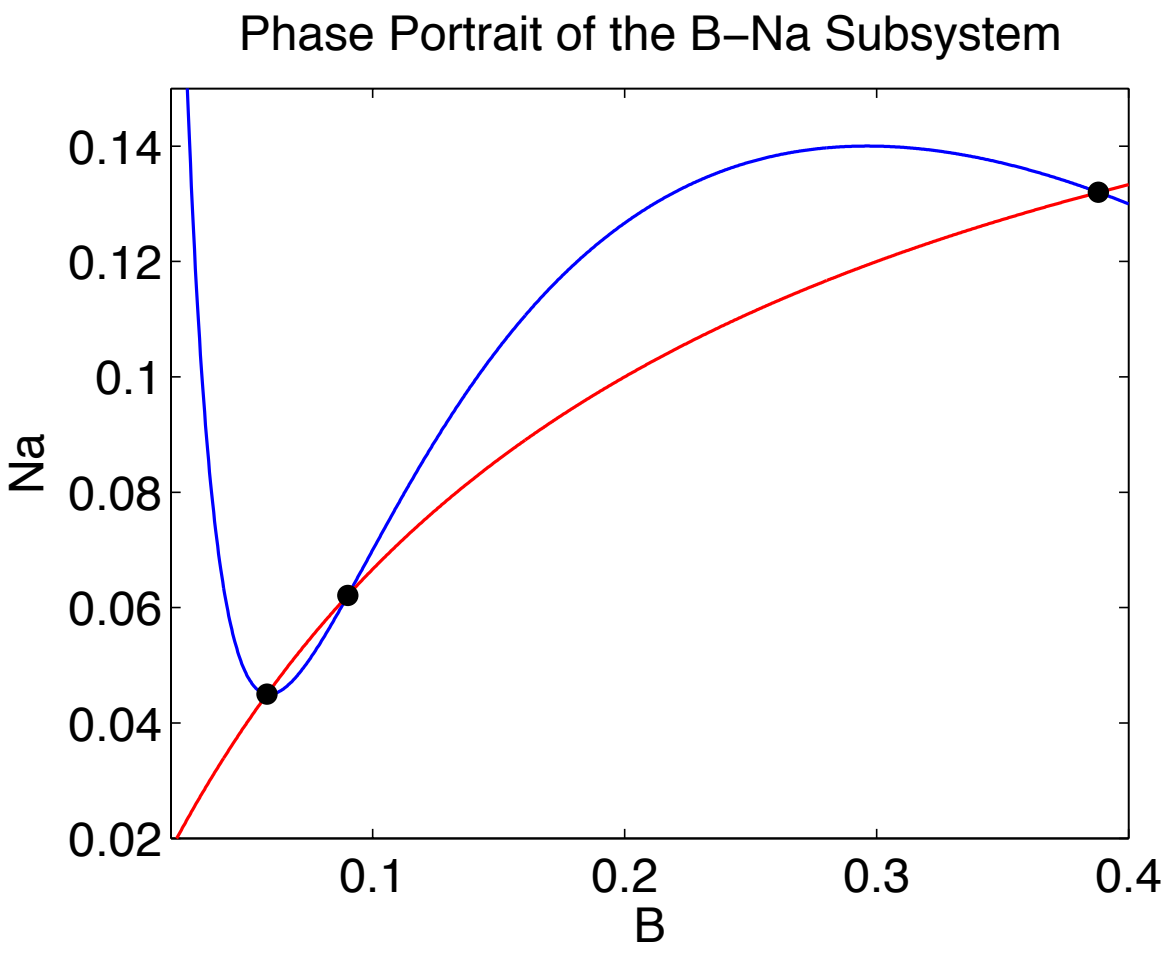

Figure 2: The nullclines of System (3.1) - (3.2). The blue nullcline shows where $\frac{dB}{dt} = 0$, and the red nullcline shows where $\frac{dN_A}{dt} = 0$. From left to right, the intersections of the blue and red lines are the equilibria (B_1, N_{A1}), (B_2, N_{A2}), and (B_4, N_{A4}).

Equilibrium	Eigenvalue 1	Eigenvalue 2	Equilibrium Type
(B_1, N_{A1})	-0.996501	-0.003829	Stable Node
(B_2, N_{A2})	-0.995730	0.002854	Saddle Point
(B_4, N_{A4})	-0.995466	-0.010759	Stable Node

Table 4: The coordinates, eigenvalues, and description of the stability for each equilibrium of the B-N_A subsystem.

Now we will check the stability of the three equilibria (B_1, N_{A1}), (B_2, N_{A2}), and (B_4, N_{A4}). Let $f_1(B, N_A)$ be the right side of Equation (3.1), and let $f_2(B, N_A)$ be the right side of Equation (3.2). The linearization of System (3.1) - (3.2) is represented by the matrix J in Equation (3.11).

$$J(B, N_A) = \begin{bmatrix} \frac{\partial f_1(B,N_A)}{\partial N_A} & \frac{\partial f_1(B,N_A)}{\partial B} \\ \frac{\partial f_2(B,N_A)}{\partial N_A} & \frac{\partial f_2(B,N_A)}{\partial B} \end{bmatrix} = \begin{bmatrix} -1 & \frac{1}{(1+sB)^2} \\ -\xi B & k_{pg}(1-2B) - \frac{\mu_1\mu_2}{(\mu_2+B)^2} - \xi N_A \end{bmatrix} \tag{3.11}$$

The eigenvalues of this system, λ_1, λ_2 satisfy

$$\det(J - \lambda I_{2x2}) = 0 \tag{3.12}$$

$$\Rightarrow \lambda^2 + \lambda \left(1 - k_{pg}(1-2B) + \frac{\mu_1\mu_2}{(\mu_2+B)^2} + \xi N_A\right) - \tag{3.13}$$

$$k_{pg}(1-2B) + \frac{\mu_1\mu_2}{(\mu_2+B)^2} + \xi N_A + \frac{\xi B}{(1+sB)^2} = 0, \tag{3.14}$$

where I_{2x2} is the identity matrix with two rows and two columns. The eigenvalues of System (3.1) - (3.2) at the first-quadrant equilibria are summarized in Table 4. As desired, the choice of parameters in Table 2 gives us a subsystem with one saddle point in between two stable equilibria. This yields the desired bistability of the model.

3.2 THE EFFECT OF PARAMETER ξ ON THE BISTABILITY OF THE B-N_A SUBSYSTEM

Before introducing IL-10 and the possibility of neutrophil paralysis into our model, we will observe the effect of varying the parameter ξ on the bistability of the B-N_A Subsystem, given by Equations (3.1) and (3.2). The parameter ξ represents the rate at which activated neutrophils are able to clear bacteria with which they come into contact. For the bifurcation diagram of B versus ξ shown in Figure 3, we see that for low values of ξ, the amount of bacteria remains at a high level and cannot return to a lower level, regardless of the initial conditions. The upper branch in the bifurcation diagram represents a state of chronic infection. If ξ increases past $\xi = 0.09294$, a lower and middle branch appear. The points on the unstable portion of the lower branch are unstable spirals, and the points on the middle branch are saddle points.

When ξ increases past $\xi = 0.09759$, a subcritical Andronov-Hopf bifurcation occurs, transforming the equilibria on the bottom branch from unstable spirals to stable spirals. When $\xi \in (0.09759, 0.1182)$, it is possible for B to go to the chronic state or the lower state of health. When ξ increases past $\xi = 0.1182$, a subcritical Andronov-Hopf bifurcation occurs, transforming points on the top branch from stable spirals to unstable spirals. For $\xi \in (0.1182, 0.1267)$, the bacteria level could settle at the health state since all other equilibria are unstable, or the system could produce oscillations. For $\xi > 0.1267$, the health state is the only equilibrium in the system.

We see that by varying ξ, we can alter the bistability of System (3.1) - (3.2). A decrease in ξ represents an immune system that is less effective at ridding the lower respiratory tract of bacteria; it makes sense that lowering ξ leads to an immune system that can only exist at a state of chronic infection and inflammation. In the next section, we introduce IL-10 and neutrophil paralysis to the system. The increase in IL-10 from the IAV infection causes the quantity of activated neutrophils to decrease, which has a similar effect on the immune system as decreasing the value of ξ in the B-N_A system; both changes represent a weakening in the immune system's ability to fight off bacterial infection and return to a healthy equilibrium.

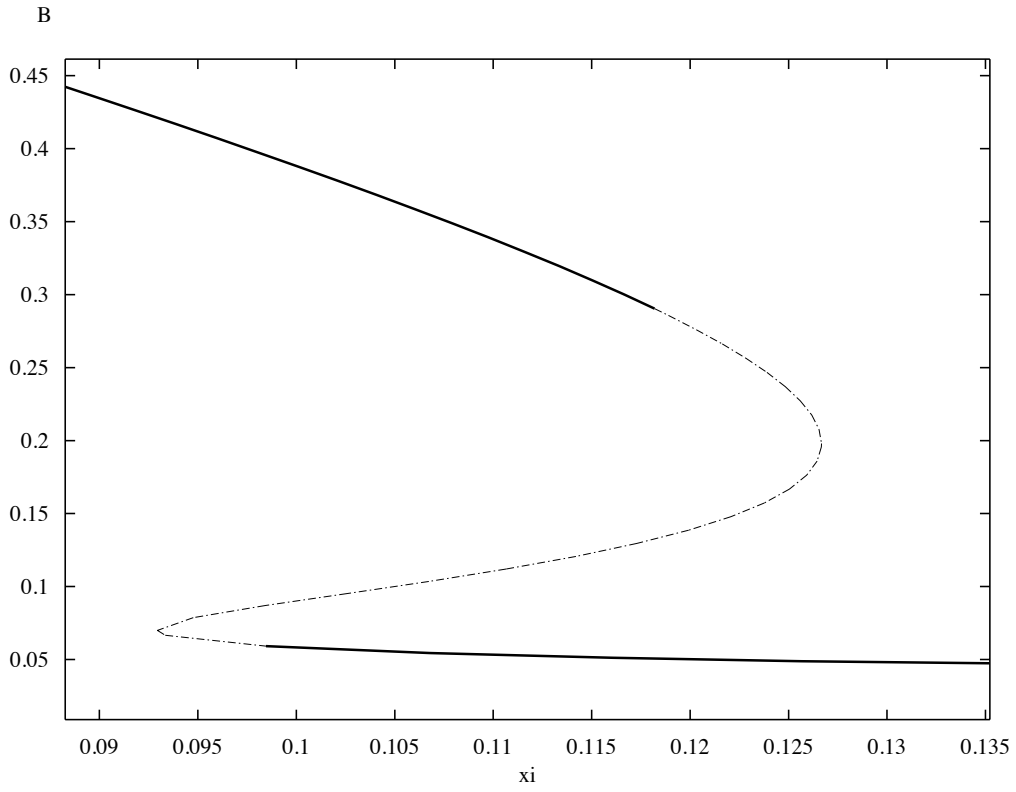

Figure 3: The Bifurcation diagram of B versus ξ for the parameter values given in Table 2. There is a parameter regime of ξ for which both health and chronic states exist and are stable. Outside of this regime, the system must stay at either health or chronic infection. On the upper and lower branch, stability changes through subcritical Andronov-Hopf bifurcations.

3.3 THE ADDITION OF THE EFFECTS OF IL-10

Now we will consider the effects of anti-inflammatory mediators, specifically IL-10, on the interaction between bacteria and activated neutrophils. As mentioned in Section 2.2.3, IL-10 has been observed to cause the inhibition of neutrophil migration to the site of infection. In our model, N_P refers to a neutrophil that has been inhibited from migrating to the site of infection by IL-10. N_A refers to a neutrophil that is able to migrate to the site of infection, where it fights off the bacteria and produces IL-10. Although there are theories as to the mechanisms of neutrophil paralysis, it is not known what all contributes to this phenomenon [1]. For this reason, we simplify the process of neutrophil paralysis by describing it in terms of interactions between neutrophils and IL-10.

We assume that an interaction between IL-10 and an activated neutrophil prevents the neutrophil from getting to the site of infection; the activated neutrophil becomes a paralyzed neutrophil. Since the IL-10 produced in response to the bacterial infection, as well as that produced from the IAV infection, will trigger neutrophil paralysis, we include effects from both sources of IL-10 in the neutrophil paralysis reaction. From the data point in Figure 1 plotted at $t = 0$, we know that the level of IL-10 pre-IAV infection is 80.46 pg/mL. The function I_{IAV} is the difference between the piecewise-linear interpolation of the first seven IL-10 data points seen in Figure 1 and 80.46, i.e. I_{IAV} is the additional IL-10 produced by the pro-inflammatory wave in response to the IAV infection. We assume also that the neutrophil paralysis is temporary and that the affected neutrophil will return to an active state before natural death. IL-10 is also assumed to eventually decay. Since I_{IAV} is the excess IL-10 above the healthy steady state caused by IAV infection, $I_{IAV}(t) = 0$ outside of the time during which the influenza infection takes place, meaning that we do not need to account for its decay. Table 5 summarizes these reactions.

Since the pro-inflammatory wave initiates the anti-inflammatory wave of the immune response, we represent the recruitment of IL-10 by activated neutrophils to the site of infection with the term $\frac{\zeta_1 N_A}{1+\zeta_2(I+I_{IAV}(t))}$. This term is appropriate since an abundance of IL-10 at the site of infection causes IL-10 production to saturate for a fixed level of activated neutrophils. The model resulting from the above assumptions and the reactions in Tables 1 and 5 is given

$N_A + I \xrightarrow{\gamma} N_P + I$	N_A is turned into N_P at rate γ when it interacts with I.
$N_A + I_{IAV} \xrightarrow{\gamma} N_P + I_{IAV}$	N_A is turned into N_P at rate γ when it interacts with I_{IAV}.
$N_P \rightarrow N_A$	N_P will turn back into N_A.
$I \xrightarrow{\eta}$	I decays at rate η.

Table 5: The interactions among N_A, N_P, and I

by System (3.15) - (3.18)

$$\frac{dN_P}{dt} = (\gamma(I + I_{IAV}(t))N_A - N_P)\,\epsilon_{N_P} \tag{3.15}$$

$$\frac{dN_A}{dt} = \left(-N_A + \frac{B}{1+sB}\right)\epsilon_{N_A} - (\gamma(I + I_{IAV}(t))N_A - N_P)\,\epsilon_{N_P} \tag{3.16}$$

$$\frac{dB}{dt} = \left(p + k_{pg}B(1-B) - \frac{\mu_1 B}{\mu_2 + B} - \xi B N_A\right)\epsilon_B \tag{3.17}$$

$$\frac{dI}{dt} = \left(\frac{\zeta_1 N_A}{1 + \zeta_2(I + I_{IAV}(t))} - \eta I\right)\epsilon_I \tag{3.18}$$

The parameters ϵ_{N_P}, ϵ_{N_A}, ϵ_B, and ϵ_I are time-scaling parameters included in order to obtain system dynamics as close to scientific observation as possible.

In order to choose the remaining parameters, we must make more assumptions while taking into account what we know to be true from experimental observation. Since health must be a possible steady state of System (3.15) - (3.18),

$$\frac{dN_P}{dt} = 0 \tag{3.19}$$

$$I_{IAV}(t) \equiv 0 \text{ during health} \Rightarrow (\gamma I N_A - N_P)\,\epsilon_{N_P} = 0 \tag{3.20}$$

$$\Rightarrow \gamma I N_A - N_P = 0 \tag{3.21}$$

$$\Rightarrow \gamma = \frac{N_P}{I N_A}. \tag{3.22}$$

We will assume that the level of activated neutrophils is equal to the level of paralyzed neutrophils during the state of health. From this assumption and the fact that the level of IL-10 at the healthy state is $I(0) = 80.46$, we have that $\gamma = \frac{1}{80.46} \approx 0.01243$. We will choose $\zeta_2 = 0.001$; since ζ_2 is multiplied by I, which takes on values much larger than those of N_A, making ζ_2 too large will cause the term $\frac{\zeta_1 N_A}{1+\zeta_2 I}$ to have little effect on the dynamics of I.

The motivation for the development of System (3.15) - (3.18) is to obtain a model supporting the hypothesis that the second hill in the IL-10 data in Figure 1 results from secondary bacterial infection in the host and that this secondary bacterial infection occurs as a result of immune dynamics triggered by the primary IAV infection.

We choose the parameters for System (3.15) - (3.18) with the following considerations in mind:

1. The bacteria most often responsible for bacterial pneumonia is *S. pneumoinae* [2], [5], [8]. *S. pneumoniae* reproduces through binary fission, doubling once every 20 to 30 minutes [12]. If we take the doubling time to be 30 minutes or $\frac{1}{48}$ days, we can solve the following differential equation to determine a value of ϵ_B.

$$\frac{dB}{dt} = \epsilon_B k_{pg} B \tag{3.23}$$

$$\Rightarrow B(t) = B_0 \exp(\epsilon_B k_{pg} t) \tag{3.24}$$

$$\Rightarrow 2B_0 = B\left(\frac{1}{48}\right) = B_0 \exp\left(\frac{\epsilon_B k_{pg}}{48}\right) \tag{3.25}$$

$$\Rightarrow \epsilon_B k_{pg} = 48 \ln(2) \approx 33.27 \tag{3.26}$$

   Since $k_{pg} = 0.05$, a result obtained in Section 3.1, we set $\epsilon_B = 665.4$.

2. *S. pneumoniae* infection occurs in the lungs one to seven days after viral infection of the upper respiratory tract [2]. We choose the time-scaling parameters ϵ_{N_A} and ϵ_{N_P} so that the bacterial infection matches this observation.

3. System (3.15) - (3.18) cannot be insensitive to the increase in IL-10 caused by the IAV infection; the dynamics of the system must be responsive to the presence of I_{IAV}.

4. The solution of System (3.15) - (3.18) should stay near the healthy equilibrium in the absence of the IAV infection. We choose parameters η and ϵ_I so that the system demonstrates these last two qualities. When finding the healthy equilibrium state, which will also serve as our set of initial conditions, we must keep the following in mind with respect to the state of health:

   a. $I_{IAV} \equiv 0$, since I_{IAV} is nonzero only in the first 9 days of IAV infection.

   b. $I \equiv 80.46$ pg/mL, since this is the amount of IL-10 shown in the IAV IL-10 data before IAV infection and since we assume that the mice are initially healthy.

   c. When we let $\xi = 0.165$ in System (3.1) - (3.2) and let all other parameters in the subsystem remain as they are in Table 2, the steady state values of B and N_A will be the same for both systems. Indeed, when System (3.15) - (3.18) is at equilibrium,

$$\frac{dN_P}{dt} = 0 \tag{3.27}$$

$$\Rightarrow \gamma(I + I_{IAV})N_A - N_P = 0 \tag{3.28}$$

$$\text{Thus } \frac{dN_A}{dt} = \left(-N_A + \frac{B}{1+sB}\right)\epsilon_{N_A} - (\gamma(I + I_{IAV})N_A - N_P)\,\epsilon_{N_P} = 0 \tag{3.29}$$

$$\Rightarrow \frac{dN_A}{dt} = \left(-N_A + \frac{B}{1+sB}\right)\epsilon_{N_A} = 0 \tag{3.30}$$

   This means that in System (3.15) - (3.18), N_A behaves as it does in the Subsystem (3.1) - (3.2). Since the dynamics of B in System (3.15) - (3.18) do not depend on any variables besides N_A, we have that the equilibrium values of B and N_A in the larger system should be the same as they are in the B-N_A Subsystem.

   d. For Equations (3.20) - (3.22), we assume that $N_A \equiv N_P$ at health.

The parameter values and initial conditions for System (3.15) - (3.18) are shown in Tables 6 and 7, respectively. Although these parameter values were selected by hand, a closer fit to the IAV IL-10 data could be obtained with the use of more sophisticated parameter estimation techniques.

Figures 4 and 5 are simulations of System (3.15) - (3.18) with the parameter values in Table 6. These simulations were run using XPPAUT and the code in the Appendix, Section

$p = 0.0012$	$k_{pg} = 0.05$	$\mu_1 = 0.01$	$\mu_2 = 0.1$
$s = 5$	$\xi = 0.165$	$\gamma = 0.01243$	$\zeta_2 = 0.001$
$\eta = 0.97$	$\epsilon_{N_P} = 0.15$	$\epsilon_{N_A} = 0.27$	$\epsilon_B = 665.4$
$\zeta_1 = 2384.48$	$\epsilon_I = 5$		

Table 6: Along with the initial conditions in Table 7, these parameter values for System (3.15) - (3.18) provide dynamics similar to those observed in the IL-10 data from Figure 1.

$B(0) = 0.0429609$
$N_A(0) = 0.03536446$
$N_P(0) = 0.03536863$
$I(0) = 80.46$

Table 7: For the parameter values in Table 6, these initial conditions for System (3.15) - (3.18) provide dynamics similar to those observed in the IL-10 data from Figure 1.

A.2. For this set of parameter values, the system yields dynamics for $I_{tot} = I + I_{IAV}$ that closely match the IL-10 data in Figure 1. Indeed, we see from Figure 4 that the dynamics of I_{tot} experience a large peak followed by a smaller, secondary peak. The first peak in I_{tot} is mostly driven by I_{IAV}; however, the dynamics occurring after the first peak are a result of the dynamics of System (3.15) - (3.18). In Figure 4, we compare I_{tot} with the IL-10 IAV data and observe the addition of I and I_{IAV} to form I_{tot}.

In Figure 5, we see that the bacterial level peaks between Day 6 and Day 7 post-IAV infection. We also observe that the level of activated neutrophils decreases between Day 2 and Day 7, while the level of paralyzed neutrophils increases during this time. These behaviors occur at the same time as the first, larger increase in IL-10 shown in Figure 1. Recall that when IL-10 levels increase, activated neutrophils are inhibited from migrating to the site of infection, allowing for bacteria at the site of infection to populate without hindrance by the activated neutrophils. The way in which I_{IAV} varies within the first 9 days post-IAV infection has the same effect on System (3.15) - (3.18) as decreasing and then increasing ξ in the Subsystem (3.1) - (3.2). In the absence of I_{IAV}, the system remains at the steady state of health, which shows that the system is reacting to the change in IL-10 resulting from the primary IAV infection.

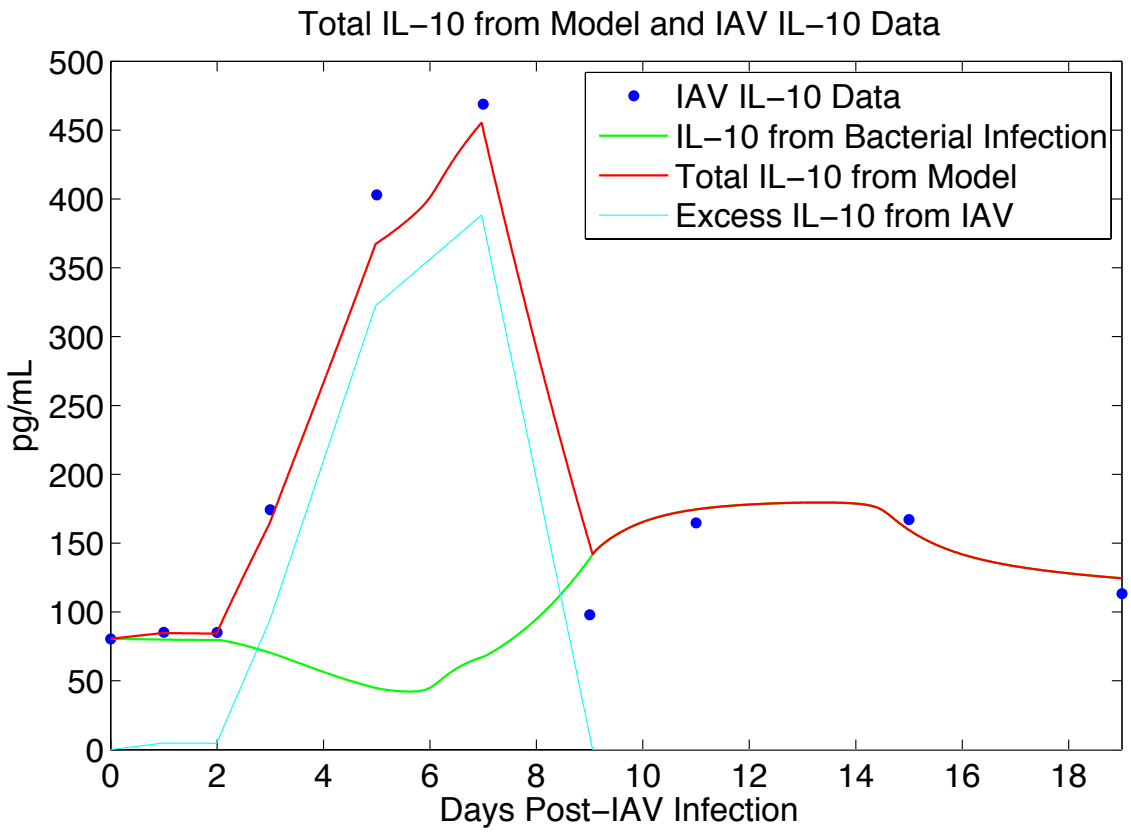

Figure 4: The dynamics of I_{tot} from System (3.15) - (3.18) closely predict the IL-10 data post IAV infection. I_{tot} is the sum of the IL-10 recruited by the bacterial infection, I, and the excess IL-10 recruited by the IAV infection, IAV.

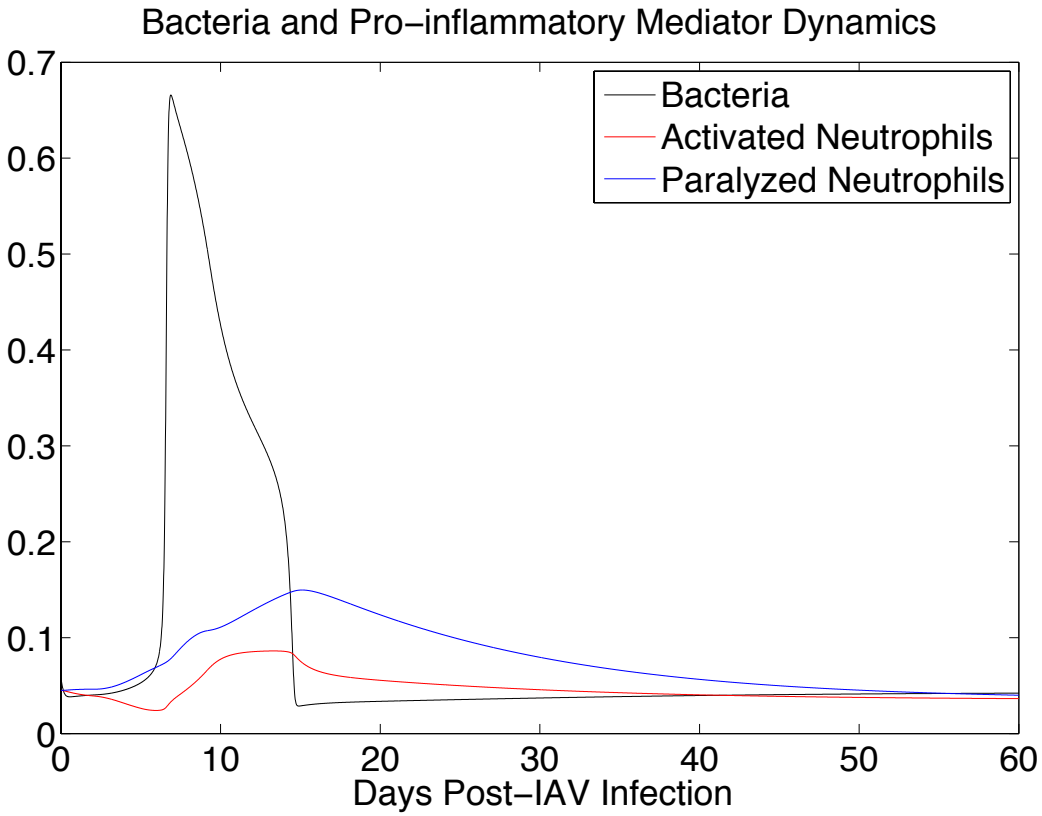

Figure 5: The dynamics of B, N_A, and N_P from System (3.15) - (3.18) demonstrates timing similar to that observed experimentally.

4.0 MODEL 2: STOCHASTIC INHALATION OF BACTERIA

4.1 DEVELOPMENT OF MODEL 2

We have developed a model for an immune system with output that is qualitatively realistic and produces IL-10 levels similar to the data collected by Toapanta et al. For this model, the rate of inhalation of bacteria into the lower respiratory tract is represented by a constant; however, the flow of bacteria into the lower respiratory tract is not constant. Instead, small quantities of bacteria are inhaled many times per day. In this next model, we assume that the same amount of bacteria is inhaled for every inhalation of bacteria and that the inhalation of bacteria is a Poisson process. With this change, we have the model represented by the System (4.1) - (4.4).

$$\frac{dN_P}{dt} = \left(\gamma(I + I_{IAV}(t))N_A - N_P\right)\epsilon_{N_P} \tag{4.1}$$

$$\frac{dN_A}{dt} = \left(-N_A + \frac{B}{1+sB}\right)\epsilon_{N_A} - \left(\gamma(I + I_{IAV}(t))N_A - N_P\right)\epsilon_{N_P} \tag{4.2}$$

$$\frac{dB}{dt} = \left(k_{pg}B(1-B) - \frac{\mu_1 B}{\mu_2 + B} - \xi B N_A\right)\epsilon_B + p_1(t) \tag{4.3}$$

$$\frac{dI}{dt} = \left(\frac{\zeta_1 N_A}{1 + \zeta_2(I + I_{IAV}(t))} - \eta I\right)\epsilon_I \tag{4.4}$$

$$p_1(t) = b_1 \sum_{i=1}^{n} \delta(t - \tau_i),$$

where δ is the Dirac delta function given by

$$\delta(s) = \lim_{a \to 0} \frac{1}{2a} \exp\left(-\left|\frac{s}{a}\right|\right)$$

The waiting times $\{\tau_{i+1}-\tau_i\}$ between inhalations of bacteria are exponentially distributed with rate parameter λ. The parameter b_1 represents the amount of bacteria inhaled at each time τ_i. Some of the values for the parameters in System (4.1) - (4.4) can be taken from our work with System (3.15) - (3.18). However, the parameters involving the stochasticity of the bacterial inhalation; such as λ and p_1; as well as some of the parameters representing immune system characteristics; such as ξ, ζ_1, η, and γ; must be set. Our first step in doing so is to consider that the average influx of bacteria in the stochastic system should be the same as the influx of bacteria in the deterministic system, i.e. $\hat{p_1}$ in System (4.1) - (4.4) should equal $\epsilon_B p$ in System (3.15) - (3.18).

Note that the expected value of the function $p_1(t)$ over a given time interval $[0, T]$ is

$$\hat{p_1} = \frac{b_1 \langle n \rangle (T)}{T},$$

where $\langle n \rangle (T)$ is the expected number of times that $p_1(t)$ is nonzero for $t \in [0, T]$. Since the number of times for which $p_1(t) \neq 0$ is a Poisson process,

$$\langle n \rangle (T) = \int_0^T \lambda dt = \lambda T \tag{4.5}$$

$$\Rightarrow \hat{p_1} = \frac{b_1 \lambda T}{T} = b_1 \lambda \tag{4.6}$$

Since we assume $\hat{p_1} = \epsilon_B p$, we obtain that

$$\epsilon_B p = b_1 \lambda \Rightarrow b_1 = \frac{\epsilon_B p}{\lambda} = \frac{0.0012(665.4)}{\lambda} = \frac{0.79848}{\lambda}$$

We will assume that the values of parameters ϵ_B, ϵ_{N_A}, ϵ_{N_P}, ϵ_I, s, k_{pg}, μ_1, μ_2, and ζ_2 are the same as in Table 6. We will find new values for the parameters λ, ζ_1, η, γ, and ξ for the stochastic model such that we observe the following behaviors:

1. In the absence of IL-10 from IAV infection, the IL-10 level in the model remains around the baseline level of 80.46 pg/mL and does not jump spontaneously.

2. In an experiment by W. J. Doyle in which humans were experimentally infected with influenza, 15% of the subjects were found to be nasopharyngeally infected with *S. pneumoniae* 6 days post viral challenge [2]. We will attempt to find parameters so that there is a 0.15 probability of a bacterial infection, by which we mean a jump in the bacteria level from the baseline level of 0.04 cfu to at least 0.2 cfu.
3. The average of the IL-10 trajectories and the IAV IL-10 data agree at most if not all of the IAV IL-10 data points.

Each of the IL-10 data points shown in Figure 1 is an average of IL-10 counts from six mice, all of which had to be euthanized in order to obtain these results. This means that the data collected by Toapanta et al. represents an average of immune system dynamics, across different immune systems. We assume that the mice in the experiment had identical immune systems, and observe whether or not System (4.1) - (4.4) exhibits the three behaviors listed above at a given parameter point by running the simulation 100 times and averaging the solutions. In order to find numerical solutions of this system, we used XPPAUT with the code found in Appendix A.3.

Although Behaviors 1 and 2 are important in finding a good parameter fit for System (4.1) - (4.4), Behavior 3 represents the primary goal of Section 4 - to develop a model supporting the hypothesis that bacterial superinfection is responsible for the small, secondary hump in the IAV IL-10 data. (See Figure 1.) To check that the system exhibits Behavior 3 at a given parameter point, we find the average of the solutions $I_{tot} = I_{IAV} + I$ and compare it to the IAV IL-10 data.

Figure 6 shows the results of five consecutive simulations of System (4.1) - (4.4) at the parameter values specified in Table 8. It is clear from the figure that the steady state level for I for these parameter values is close to 96 as opposed to being near 80.46, so System (4.1) - (4.4) does not completely satisfy Behavior 1 at the given parameter point, although the chance of a spontaneous bacterial infection is very low. Furthermore, for this parameter point, the probability that bacterial infection occurs is 0.52, so System (4.1) - (4.4) also does not satisfy Behavior 2 at the given parameter point.

However, System (4.1) - (4.4) does satisfy Behavior 3. In Figure 7, the average of I_{tot} over 100 trials is compared to the IAV IL-10 data. From this plot, we see that I_{tot} matches

$\epsilon_B = 665.4$	$\epsilon_{N_P} = 0.15$	$s = 5$	$\epsilon_{N_A} = 0.27$
$\epsilon_I = 15$	$k_{pg} = 0.05$	$\mu_1 = 0.01$	$\mu_2 = 0.1$
$\zeta_2 = 0.001$	$b_1 = \frac{\epsilon_B p}{\lambda}$	$\lambda = 600$	$\zeta_1 = 2305$
$\xi = 0.161$	$\eta = 0.78$	$\gamma = 0.0048$	

Table 8: The parameter values for System (4.1) - (4.4) that yield the results seen in Figures 6, 7, and 8.

the trend established by the IAV IL-10 data points. In Figure 8, we see the average dynamics of bacteria, activated neutrophils, and paralyzed neutrophils corresponding to the 100 trials from which the average I_{tot} in Figure 7 was found. We see that that the bacteria does not peak as high as it does for System (3.15) - (3.18) in Figure 5, but this makes sense because these are dynamics over trials for which bacterial infection did or did not occur. For example, Figure 9 shows the dynamics of B, N_A, and N_P for a trial for which there was bacterial infection, while Figure 10 shows the solutions to the same variables for a trial for which no bacterial infection occurred.

This model with stochastic bacteria inhalation is more realistic than the model with constant rate of bacterial inhalation because it demonstrates the possibility of bacterial infection occurring with an assigned probability. In System (3.15) - (3.18), the parameter values determine fully whether or not the immune system will be able to contain the bacteria before infection can occur, but we know from experience that hosts with healthy immune systems do not obtain lower-respiratory tract infections never or always; there is some chance of getting sick, but there is no certainty of contracting a bacterial infection or not.

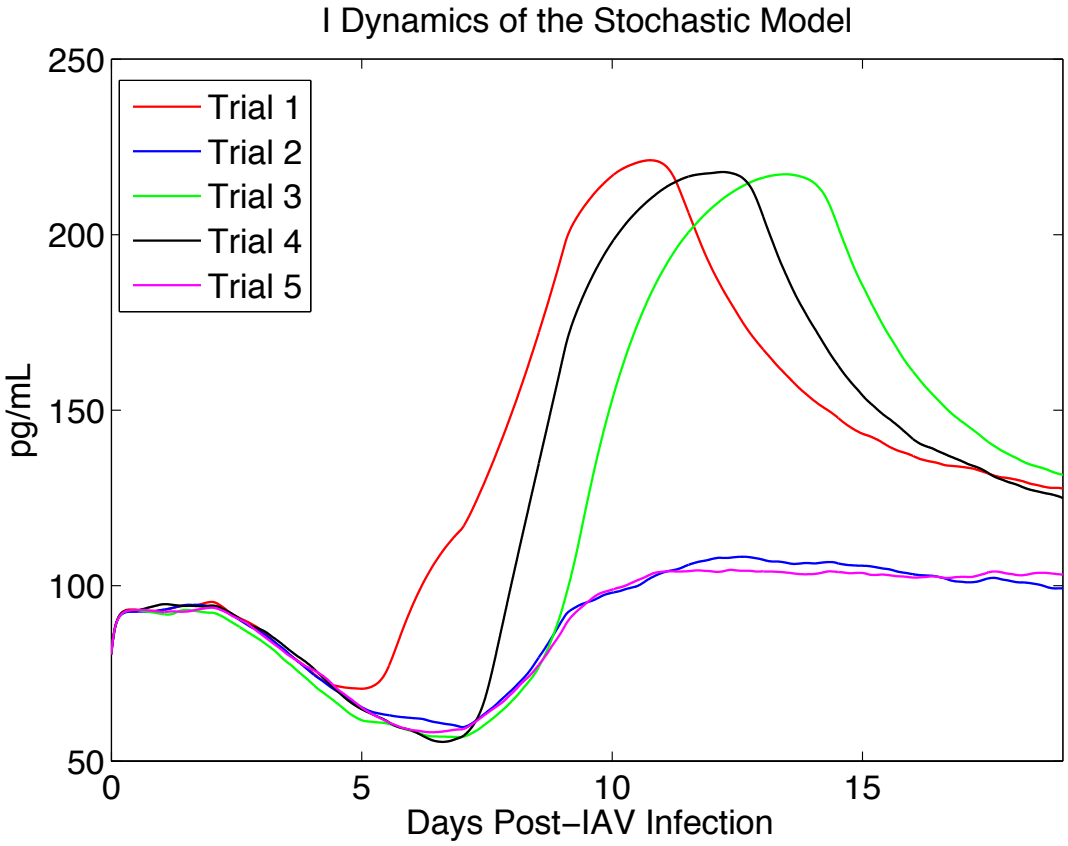

Figure 6: The dynamics of I for five different trials of System (4.1) - (4.4).

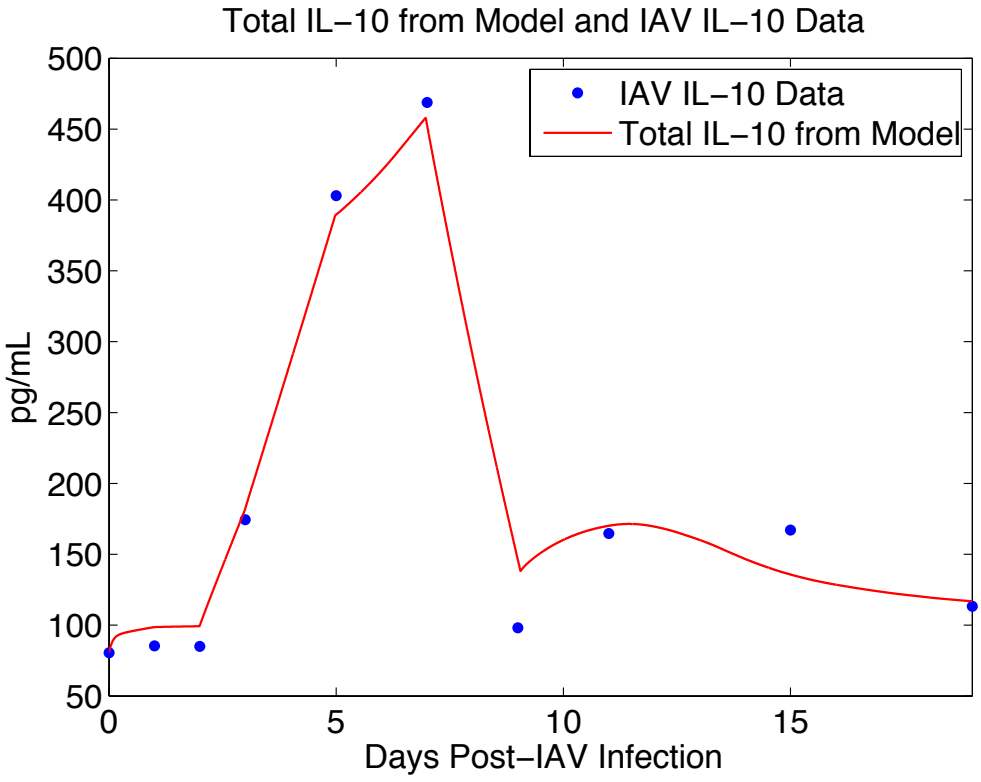

Figure 7: The average over 100 trials of I_{tot} from System (4.1) - (4.4) and the IAV IL-10 data.

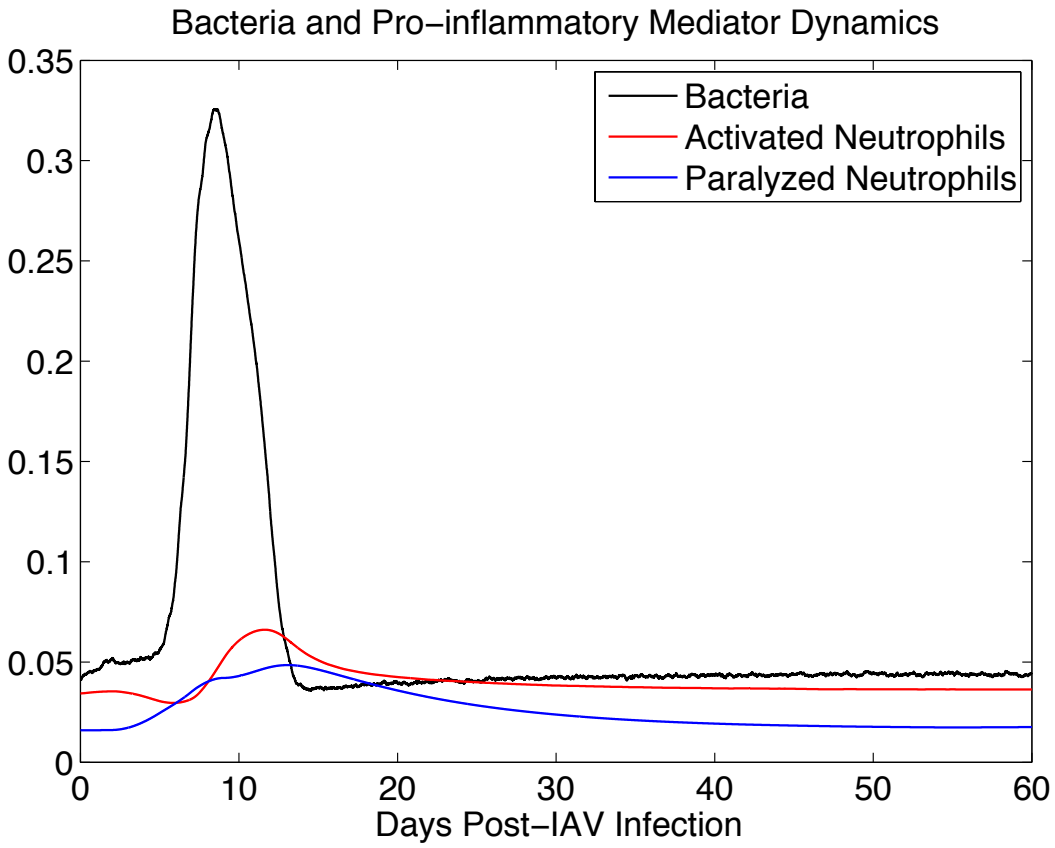

Figure 8: The dynamics of B, N_A, and N_P from System (4.1) - (4.4). The maximum average bacteria level is lower than the maximum bacteria level obtained from the parameter selection for System (3.15) - (3.18). (See Figure 5.)

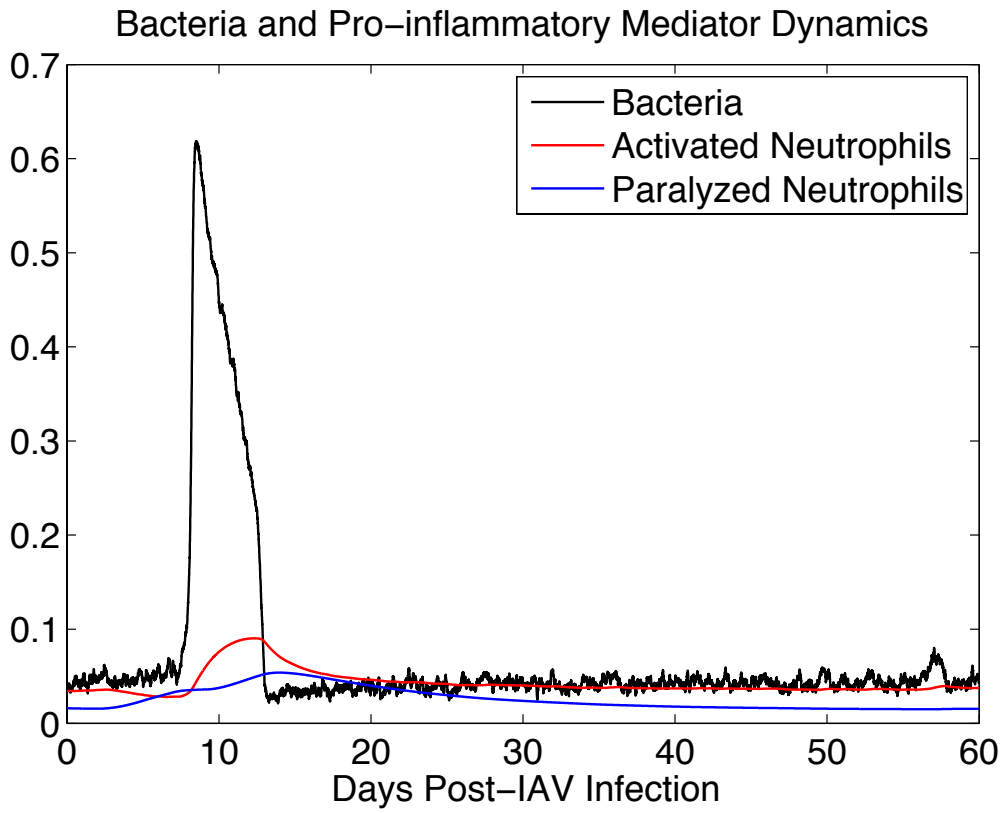

Figure 9: The dynamics of B, N_A, and N_P from System (4.1) - (4.4) for a trial during which bacterial infection occurred.

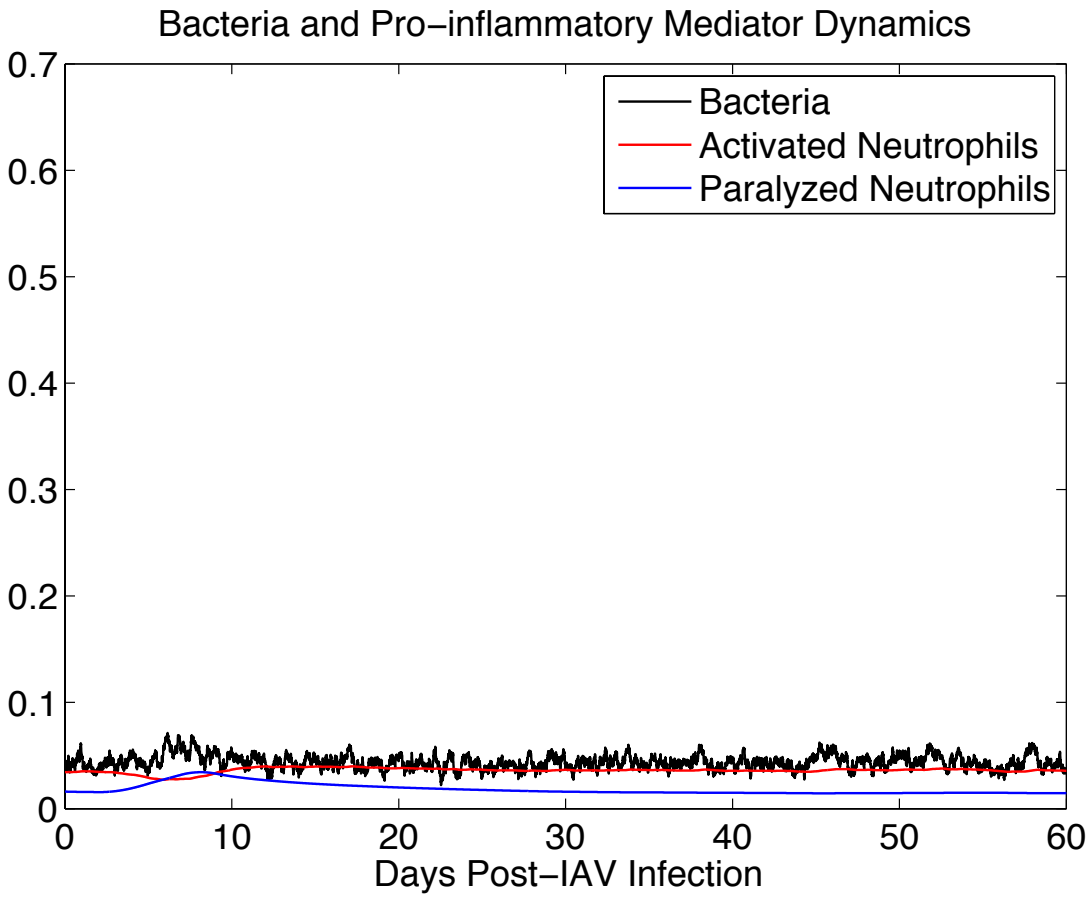

Figure 10: The dynamics of B, N_A, and N_P from System (4.1) - (4.4) for a trial during which bacterial infection did not occur.

4.2 CONTRIBUTING FACTORS TO BACTERIAL INFECTION IN MODEL 2 SOLUTION

Notice from Figure 6 that the solution to System (4.1) - (4.4) will fall under two distinct cases, one of which results in bacterial infection, and one of which does not. We wish to determine the factors that contribute to whether or not the solution results in bacterial infection. After observing many simulations System (4.1) - (4.4), one observes that when bacterial infection does occur in the solution, it occurs within the approximate time window between Day 4 and Day 8. Figure 11 shows a plot of $B(t)$ for four simulations of the System, one of which does not result in bacterial infection and three of which do, and Figure 12 shows the mean $B(t)$ among cases of bacterial infection and the mean $B(t)$ among cases of health.

The dependence on the occurrence of bacterial infection on the time window of Day 4 to Day 8 suggests that there is some aspect of the System that makes a sudden jump in bacteria levels possible during this time period and highly improbably outside of the time period. In Figure 13, we see a plot of $I_{IAV}(t)$, the excess IL-10 produced in response to the IAV infection. During the time window from Day 4 to Day 8, $I_{IAV}(t) \approx 200$ or greater. However, $I_{IAV}(t) \approx 200$ does not guarantee that the solution to the System exhibits bacterial infection since it is possible for the System to remain at health despite the temporary increase in levels of $I_{IAV}(t)$.

We wish to examine the effect of $I_{IAV}(t)$ on System (4.1) - (4.4). To do so, we make some assumptions in order to reduce the deterministic model, System (3.15) - (3.18), to a one-dimensional ODE. Since we would like to compare the results of this analysis to the stochastic model with the parameters in Table 8, we will consider the deterministic model with the parameter values in Table 8 relevant to System (3.15) - (3.18).

First, we replace $I_{IAV}(t)$ with a constant parameter called IAV so that we can explicitly observe the effects of different values of $I_{IAV}(t)$ on the occurrence of bacterial infection. This yields the system of differential equations, System (4.7) - (4.10).

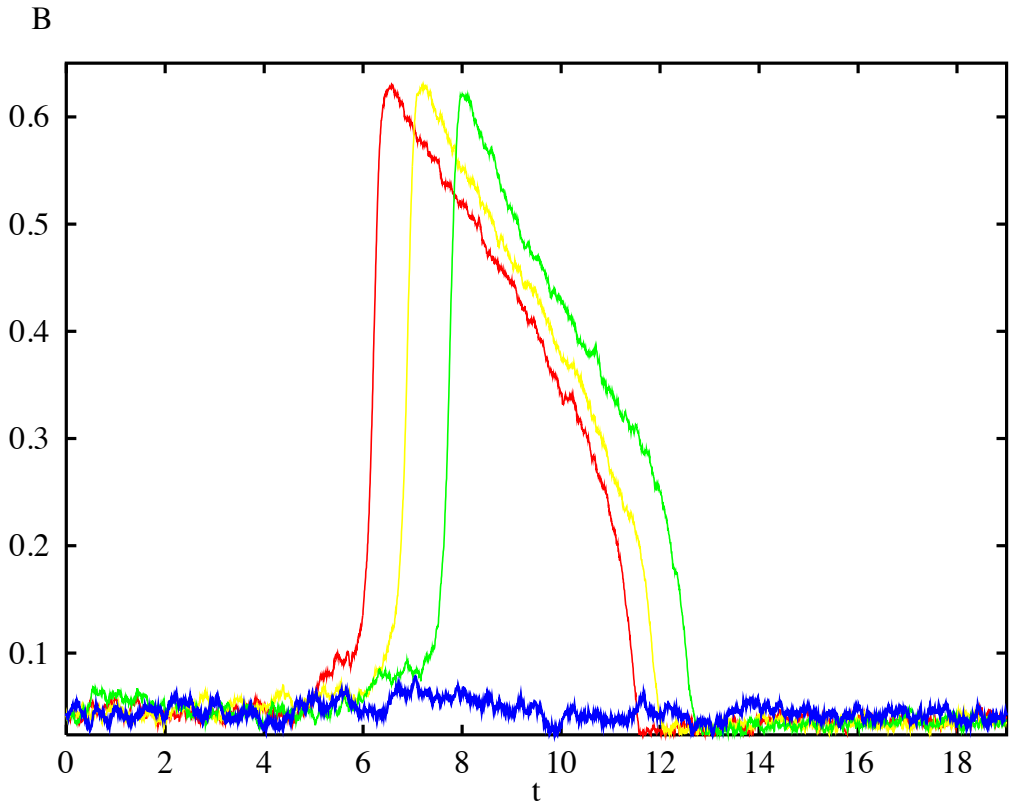

Figure 11: Four simulations of System (4.1) - (4.4). The three simulations that do result in bacterial infection are representative of most other simulations of the System that result in infection in that bacterial infection does not occur outside of an approximate time window from Day 4 to Day 8. (See Figure 12 for the mean of $B(t)$ from 30 simulations for which bacterial infection occurred.) From Figure 13, we see $I_{IAV}(t) \approx 200$ or greater in this time window.

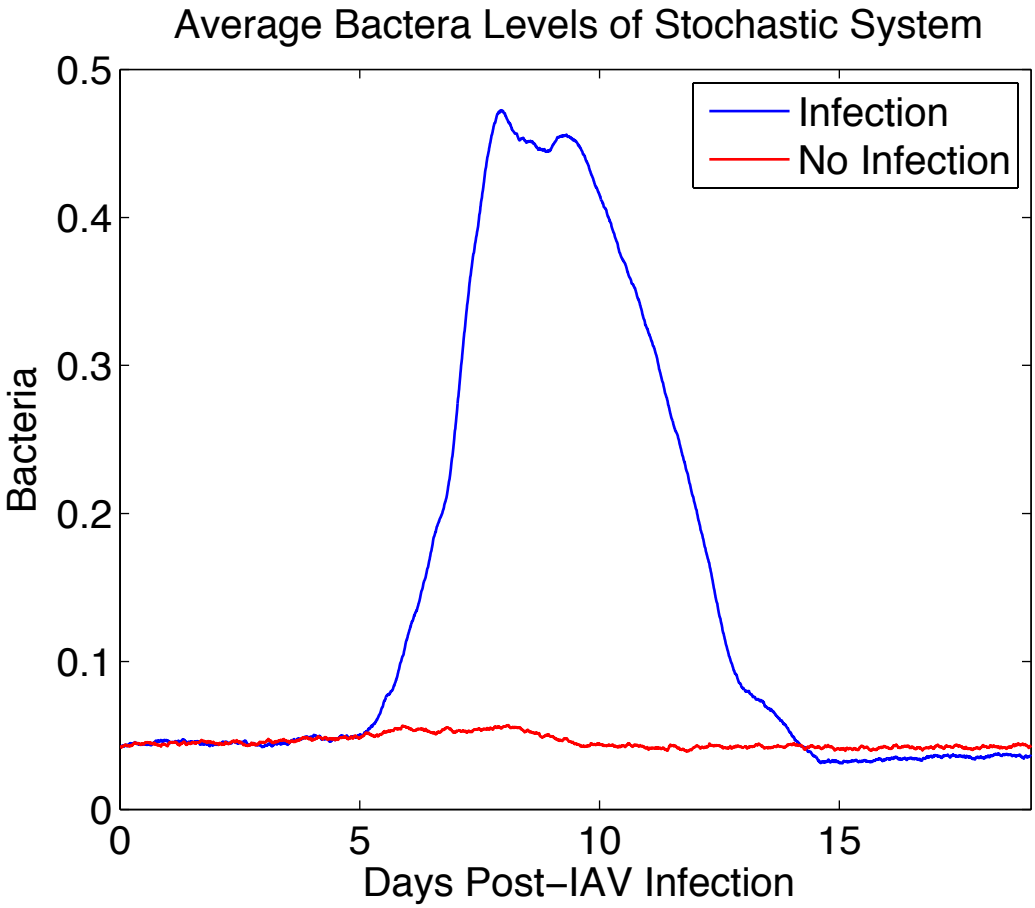

Figure 12: The mean of $B(t)$ from 30 simulations of System (4.1) - (4.4) for which bacterial infection does occur and the mean over 30 simulations for which bacterial infection does not occur.

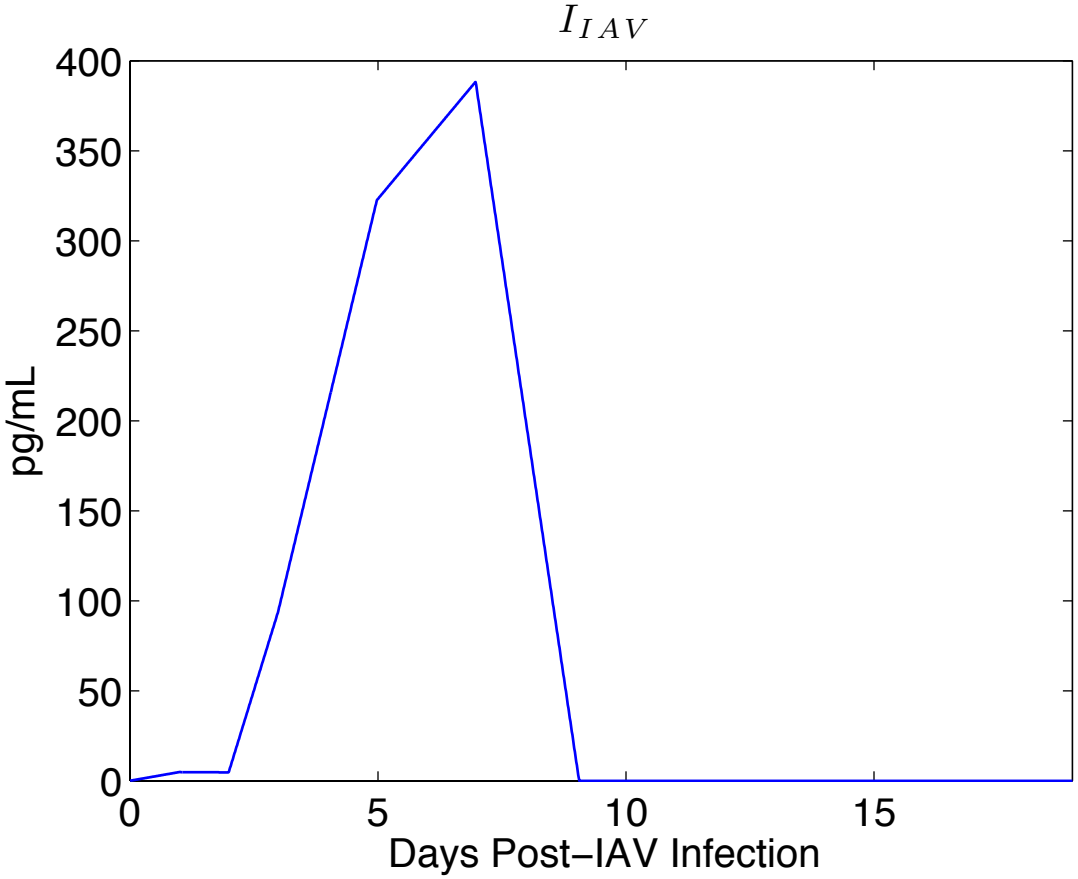

Figure 13: A plot of $I_{IAV}(t)$, the additional IL-10 produced as a result of the IAV infection.

$$\frac{dN_P}{dt} = (\gamma(I + IAV)N_A - N_P)\,\epsilon_{N_P} \tag{4.7}$$

$$\frac{dN_A}{dt} = \left(-N_A + \frac{B}{1+sB}\right)\epsilon_{N_A} - (\gamma(I + IAV)N_A - N_P)\,\epsilon_{N_P} \tag{4.8}$$

$$\frac{dB}{dt} = \left(p + k_{pg}B(1-B) - \frac{\mu_1 B}{\mu_2 + B} - \xi B N_A\right)\epsilon_B \tag{4.9}$$

$$\frac{dI}{dt} = \left(\frac{\zeta_1 N_A}{1 + \zeta_2(I + IAV)} - \eta I\right)\epsilon_I \tag{4.10}$$

As we change the values of parameter IAV, we observe that $I \in [72.92, 96.16]$ for System (4.7) - (4.10); we let $I \equiv 96.16$, the steady state value at health $I(0)$, since the extent to which I changes is small compared to the extent to which IAV changes. $I \equiv 96.16$ means that the parameter IAV must take on values in the interval $[0, 372.48]$ because $I_{tot} = I_{IAV}(t) + I$ must take on values in $[0, 468.46]$. Also, note that $N_{tot}(0) = N_A(0) + N_P(0) = 0.052$ and that $N_{tot} \in [0.052, 0.111]$; we let $N_{tot} \equiv 0.052$. Observe the following.

$$0 = \frac{dN_P}{dt} = (\gamma((IAV)N_A - N_P))\,\epsilon_{N_A} \tag{4.11}$$

$$\Rightarrow N_P = \gamma(IAV)N_A \tag{4.12}$$

This yields

$$N_{tot} = N_A + N_P \tag{4.13}$$

$$\Rightarrow N_{tot} = N_A + \gamma(IAV)N_A \tag{4.14}$$

$$\Rightarrow N_A = \frac{N_{tot}}{1 + \gamma(IAV)} \tag{4.15}$$

Plugging this value of N_A into $\frac{dB}{dt}$, we obtain

$$\frac{dB}{dt} = \left(p + k_{pg}B(1-B) - \frac{\mu_1 B}{\mu_2 + B} - \frac{\xi N_{tot} B}{1 + \gamma(IAV)}\right)\epsilon_B \tag{4.16}$$

We set $\frac{dB}{dt} = 0$ and solve for B at several different values of IAV to observe how changes in IAV affect the steady state values of B. Figure 14 shows plots of the equation for several

values of IAV. For $IAV = 0$, we see that there are three equilibria - one unstable equilibrium between two stable equilibria. As IAV increases, the unstable equilibrium and the stable equilibrium to its left disappear. Figure 15 provides a closer look at this phenomenon. When IAV is below a certain value, B must be at least 0.06, or larger depending on how small IAV is, in order for it to be pulled toward the higher stable equilibrium. Otherwise, B is pulled toward the lower stable equilibrium. The value that B must be in order for it to be pulled toward the higher stable equilibrium decreases as IAV increases.

We can apply these findings to the stochastic system. From what we observed above, B must be above a necessary value dependent on the value of $I_{IAV}(t)$ in order for bacterial infection to occur. However, due to the constraints on the stochasticity of B influenced by the values of parameters b_1 and λ in System (4.1) - (4.4), the lower the value of $I_{IAV}(t)$, the more improbable is is that B will reach the necessary value needed in order to be attracted to the higher equilibrium. In other words, whether or not the solution of System (4.1) - (4.4) results in bacterial infection at a certain time t^* depends on the value of $I_{IAV}(t^*)$ and whether or not the stochasticity of the system has brought $B(t^*)$ to a large enough value so as to be pulled toward the higher equilibrium of infection.

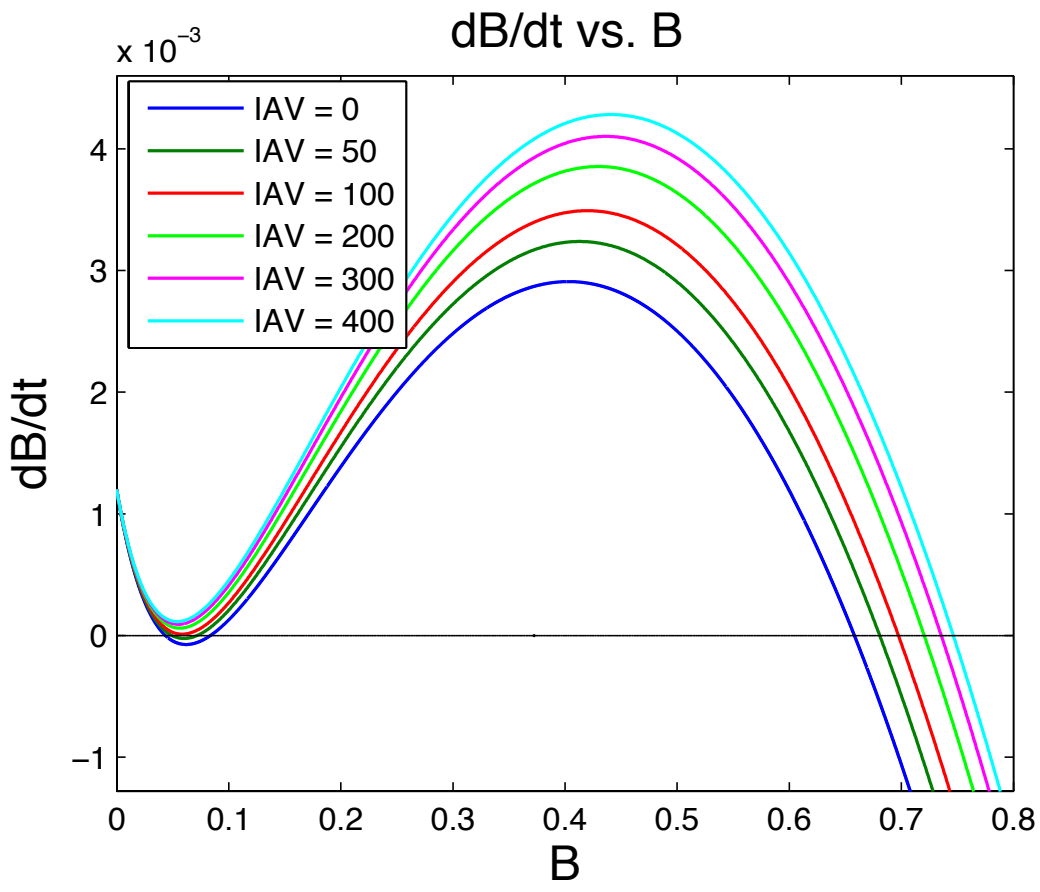

Figure 14: A plot of $\frac{dB}{dt}$, Equation (4.16), versus B for several values of IAV. The value of IAV determines the number of equilibria of Equation (4.16). See Figure 15 for a closer look at the disappearance of the left and middle equilibria as IAV increases.

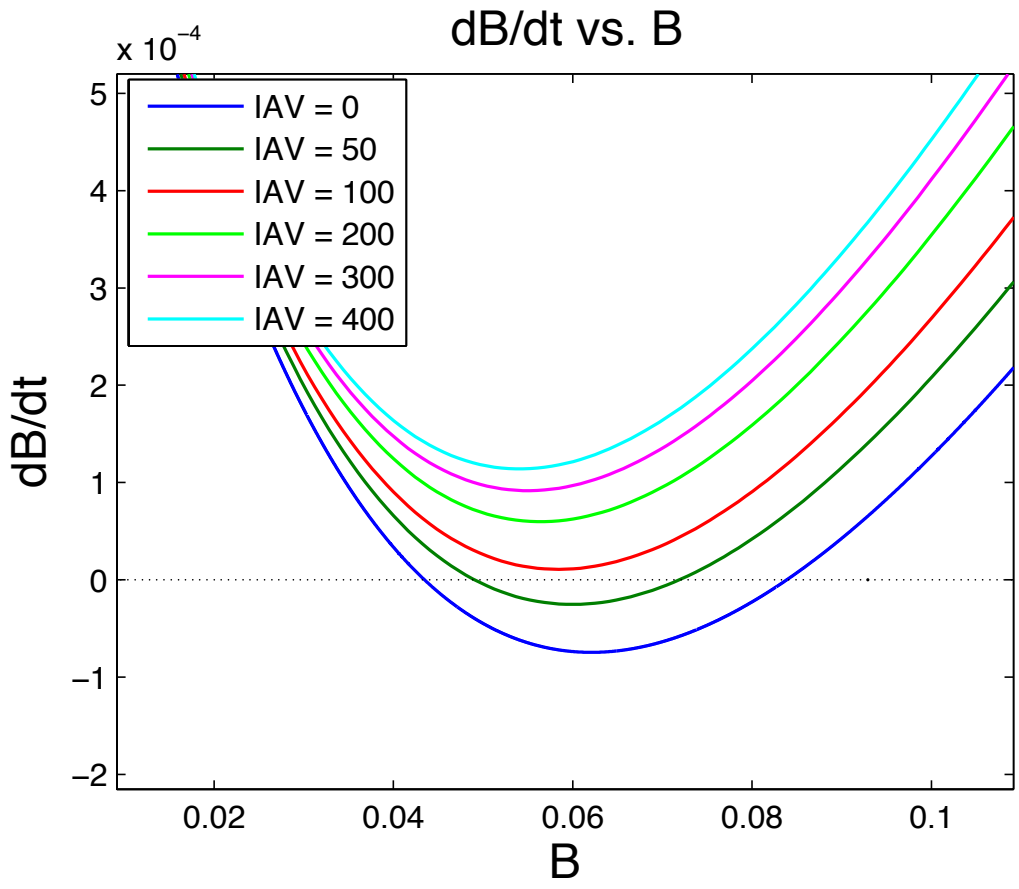

Figure 15: The left and middle equilibria of Equation (4.16) disappear as IAV increases. When $IAV < 100$, B must stochastically jump higher than the middle equilibrium in order to be pulled toward the stable equilibrium to the right. (See Figure 14.) For this reason, bacterial infection is highly unlikely to occur for $IAV < 100$.

5.0 CONCLUSION

Through the above research, we were able to develop a simple model of bacterial infection involving bacteria, neutrophils, and IL-10. We used this model to support the possibility that the unexpected secondary hump in the IAV IL-10 data collected by Toapanta et al. is due to an unintended bacterial superinfection occurring after the mice were inoculated with IAV. While we were able to find parameters for the deterministic model that satisfied all of our criterion and yielded results that matched the IL-10 data, the model with stochastic bacterial inhalation produced a more realistic infection scenario by modeling the somewhat random nature of illness and infection. In order to choose parameters that yield results exhibiting all expected behaviors, we could perform a sensitivity analysis on the parameters to find out which are worth varying and which are not in order to obtain the desired results.

One reason for the difficulty in fitting System (4.1) - (4.4) is that we are working with one specific immune system as established by our parameter point choice. It is probable that, since the IAV IL-10 data comes from many different rats, we would want to be able to vary the parameters slightly in order to obtain a wider spread of the possible immune responses. For example, for the parameter choice in Table 8, all solutions return to the healthy state state, but perhaps some of the mice were not able to recover from the bacterial infection. In this case, we would want the variation in parameters to be such that the change in IL-10 caused by the IAV infection can cause bacteria levels to jump to the high branch in Figure 3, while also being able to allow bacteria levels to stay at the lower branch. In order to obtain this, we could include stochastic variation of the parameters in a modification of System (4.1) - (4.4). We could also vary the parameter b_1 stochastically, since the host probably inhales varying amounts of bacteria as opposed to inhaling the same amount of bacteria every time bacteria is taken into the lower respiratory tract.

Finally, these models could be useful in considering the probability of contracting secondary bacterial pneumonia after an IAV infection with respect to individuals with compromised immune systems and the elderly. Community acquired pneumonia is a common complication for the elderly living in nursing homes or for chronically ill patients who spend much time in hospital intensive care units.

APPENDIX

CODE

A.1 NAB_PP.ODE CODE

```
NA'=-NA+B/(1+ss*B)
B'=p+kpg*B*(1-B)-(m1*B/(m2+B))-xi*B*NA)

par p=0.0012, kpg=0.05, m1=0.01, m2=0.1, xi=0.1, ss=5

init NA=0.0449829
init B=0.0580362

@ method=rk4, tol=1e-7, dt=0.01, total=200, bounds=1e70
@ maxstore=100000

done
```

A.2 NB_V3_C.ODE CODE

```
#Note: IL10_linear.tab is the IL-10 data minus baseline value of 80.64
table ca_ IL10_linear.tab
```

```
table caFull_ IL10_extended.tab

ca(t)=if((t<=9.0949)&(t>=0))then(ca_(qq*(t)))else(0.0)
caFull(t)=if((t<=19)&(t>=0))then(caFull_(t))else(if(t<0)then(80.46)else(113.28))

NP'=(g*K*NA-NP)*epsNp
NA'=(-NA+B/(1+ss*B))*epsNa-(g*K*NA-NP)*epsNp
B'=(p+kpg*B*(1-B)-(m1*B/(m2+B))-xi*B*NA)*epsB
K'=(ca(t)+z1*NA/(1+z2*K)-y*K)*epsK

par qq=1, epsNp=0.15, epsK=15, z1=2384.48, z2=0.001
par g=0.01243, epsNA=0.27, ss=5, y=0.97
par epsB=665.4, p=0.0012, kpg=0.05, m1=0.01, m2=0.1, xi=0.165
aux myca=ca(t)/1000
aux IL10=caFull(t)

init NP=0.03536446
init NA=0.03536446
init B= 0.0429609
init K=80.46

@ method=rk4, tol=1e-7, dt=0.01, total=60, bounds=1e70
@ maxstore=100000

done
```

A.3 NB_V5_2.ODE CODE

```
#Note: IL10_linear.tab is the IL-10 data minus baseline value of 80.64
```

```
table ca_ IL10_linear.tab
table caFull_ IL10_extended.tab
ca(t)=if((t<=9.0949)&(t>=0))then(ca_(qq*(t)))else(0.0)
caFull(t)=if((t<=19)&(t>=0))then(caFull_(t))else(if(t<0)then(80.46)else(113.28))

NP'=(g*(K+ca(t))*NA-NP)*epsNp
NA'=(-NA+B/(1+ss*B))*epsNa-(g*(K+ca(t))*NA-NP)*epsNp
B'=(p+kpg*B*(1-B)-(m1*B/(m2+B))-c*B*NA)*epsB
K'=(z1*NA/(1+z2*(K+ca(t)))-y*K)*epsK

nap'=(-nap+na)/tauf
switch'=0
switch2'=0
markov z 2
{0} {lambda}
{100000000000} {0}
global 1 z-.5 {b=b+b1}
trial'=0
par tauf=1
global 1 nap-thresh1 {switch2=switch2+1}
global -1 nap-thresh2 {switch2=switch2+1}
global 1 nap-thresh1 {switch=switch+(t>0)}
global -1 nap-thresh2 {switch=switch+(t>0)}
global 1 t-tend {out_put=1}

par thresh1=0.05, thresh2=0.045, thresh3=300, thresh4=90
par thresh5=0.5, thresh6=0.3
par lambda=600, p=0, c=0.161
par qq=1, epsNp=0.15, epsK=15, z1=2304.72, z2=0.001
par g=0.0048, epsNA=0.27, ss=5, y=0.78
```

```
par epsB=665.4, kpg=0.05, m1=0.01, m2=0.1
par tend=60.01234

b1=0.79848/lambda

only trial,switch,switch2,bzero,xi
aux bzero=b1
aux xi=c
aux IL10=caFull(t)
aux I=K+ca(t)

init NP=0.01602396
init NA=0.03433738
init B=0.04145409
init K=80.46
init switch=0
@ method=euler, tol=1e-7, dt=0.001, total=91, bounds=1e70
@ maxstore=100000, njmp=5, T0=-30
@ trans=100
@ range=1,rangereset=np,rangestep=100,rangeover=trial
@ rangelow=0,rangehigh=100
done
```

BIBLIOGRAPHY

[1] J. C. Alves-Filho, F. Spiller, and F. Q. Cunha, *Neutrophil paralysis in sepsis*, SHOCK **34**, Supplement 1, (2010).

[2] L. O. Bakaletz, *Viral potentiation of bacterial superinfection of the respiratory tract*, Trends in Microbiology **3** (1995), 110–114.

[3] G. B. Ermentrout, *Simulating, Analyzing, and Animating Dynami- cal Systems: A Guide to XPPAUT for Researchers and Students*, First Edition, Society for Industrial and Applied Mathematics, Philadelphia (2002).

[4] E. Goldstein, T. Akers, and C. Prato, *Role of immunity in viral-induced bacterial superinfections of the Lung*, Infection and Immunity **8** (1973), 757–761.

[5] R. Malley, A. M. Stack, R. N. Husson, C. M. Thompson, G. R. Fleisher, and R. A. Saladino, *Development of a model of focal pneumococcal pneumonia in young rats*, Journal of Immune Based Therapies and Vaccines **2(2)** (2004), doi:10.1186/1476-8518-2-2.

[6] J. L. McAuley, F. Hornung, K. L. Boyd, A. M. Smith, R. McKeon, J. Bennink, J. W. Yewdell, and J. A. McCullers, *Expression of the 1918 influenza A virus PB1-F2 enhances the pathgenesis of viral and secondary bacterial pneumonia*, Cell Host & Microbe **2** (2007), 240–249.

[7] J. A. McCullers, *Effect of antiviral treatment on the outcome of secondary bacterial pneumonia after influenza*, The Journal of Infectious Diseases **190** (2004), 519–526.

[8] D. M. Morens, J. K. Taubenberger, and A. S. Fauci, *Predominant role of bacterial pneumonia as a cause of death in pandemic influenza: implications for pandemic influenza preparedness*, J Infect Dis. **198** (2008), 962–970.

[9] G. Palacios, M. Hornig, D. Cisterna, N. Savji, A. V. Bussetti, V. Kapoor, J. Hui, R. Tokarz, T. Briese, E. Baumeister, and W. I. Lipkin, *Streptococcus pneumoniae coinfection is correlated with the severity of H1N1 pandemic influenza*, PLoS ONE **4(12)**:e8540, (2009), doi: 10.1371/journal.pone.0008540.

[10] L. Sun, R. Guo, M. W. Newstead, T. J. Standiford, D. R. Macariola, and T. P. Shanley, *Effect of IL-10 on neutrophil recruitment and survival after Pseudomonas aeruginosa challenge*, Am J Respir Cell Mol Biol **41** (2009), 76–84.

[11] F. R. Toapanta and T. M. Ross, *Impaired immune responses in the lungs of aged mice following influenza infection*, Respiratory Research **10** (2009).

[12] K. Todar, *Streptococcus pneumoniae*, (2011), Retrieved from http://www.textbookofbacteriology.net/S.pneumoniae.html.

[13] CDC, *Bacterial coinfections in lung tissue specimens from fatal cases of 2009 pandemic influenza A (H1N1) – United States, May – August 2009*, MMWR 2009 **58** (Early Release), 1–4.

[14] World Health Organization, *Influenza (seasonal)* [Fact sheet], (2009), Retrieved from http://www.who.int/mediacentre/factsheets/fs211/en/index.html.

[15] World Health Organization, *Ten concerns if avian influenza becomes a pandemic*, (2005), Retrieved from http://www.who.int/csr/disease/influenza/pandemic10things/en/.